Distal regulatory sequences contribute to diversity in brain oxytocin receptor expression patterns and social behavior

Qi Zhang[1,2,3,*], Luis Augusto Eijy Nagai[4], Mina Tsukamoto[1], Lenin C. Kandasamy[1], Kiyoshi Inoue[5], Maria F. Pires[1], Minsoo Shin[1], Yutaro Nagasawa[1], Tsetsegee Sambuu[1], Sonoko Ogawa[6], Kenta Nakai[7], Shigeyoshi Itohara[2], Larry J Young[3,5,8]

[1]Laboratory for Social Neural Networks, Faculty of Human Sciences, University of Tsukuba, Japan; [2]Laboratory for Behavioral Genetics, CBS, RIKEN, Japan; [3]Center for Social Neural Networks, Faculty of Human Sciences, University of Tsukuba, Japan; [4]Institute for Quantitative Biosciences, The University of Tokyo, Japan; [5]Center for Translational Social Neuroscience, Emory National Primate Research Center, Emory University, USA; [6]Laboratory of Behavioral Neuroendocrinology, Faculty of Human Sciences, University of Tsukuba, Japan; [7]Laboratory of Functional Analysis in silico, Human Genome Center, The University of Tokyo, Tokyo, Japan; [8]Department of Psychiatry and Behavioral Science, Emory University, USA.

*Correspondence: zhangqi@human.tsukuba.ac.jp or qi.zhang@a.riken.jp;

Classification: Biological Science: Neuroscience

Keywords: oxytocin system, behavioral evolution, topologically associating domain (TAD), bacterial artificial chromosome (BAC), brain, mammary gland, partner preference, maternal care, evolvability.

The PDF file includes:
Main Text
Figures 1 to 4
Supplementary Figures 1to 6, supplementary Tables 1 and 2

Summary

The oxytocin receptor (OXTR) modulates social behaviors in a species-specific manner. Remarkable inter- and intraspecies variation in brain OXTR distribution are associated with diversity in social behavior. To test the causal effect of developmental variation of OXTR expression on the diversity of social behaviors, and to investigate potential genetic mechanisms underlying the phylogenetic plasticity in brain *Oxtr* expression, we constructed BAC transgenic mice harboring the entire prairie vole *Oxtr* locus with the entire surrounding intergenic regulatory elements. Eight independent "volized" *prairie vole-Oxtr* (*pvOxtr*) mouse lines were obtained; remarkably, each line displayed a unique pattern of brain expression distinct from mice and prairie voles. Four *pvOxtr* lines were selected for further investigation. Despite robust differences in brain expression, *Oxtr* expression in mammary tissue was conserved across lines. These results and topologically associating domain (TAD) structure analysis suggest that *Oxtr* expression patterns in brain, but not other tissues, involve contributions of distal regulatory elements beyond our BAC construct. Moreover, "volized" mouse lines with different brain *Oxtr* expression patterns showed differences in partner preference and maternal behaviors. We speculate that transcriptional hypersensitivity to variable distal chromosomal sequences through long-distance interactions with proximal regulatory elements may contribute to "evolvability" of brain *Oxtr* expression. The "evolvability" of brain *Oxtr* expression constitutes a transcriptional mechanism to generate variability in brain OXTR which, through natural selection, can generate diversity in adaptive social behaviors while preserving critical peripheral expression. Transcriptional lability of brain *OXTR* expression may also contribute to variability in social phenotype in humans, including psychiatric outcomes.

Introduction

Brain oxytocin receptors (OXTR) regulate a wide range of social behaviors including social recognition, maternal care, social bonding, empathy related behaviors, and aggression [1-3]. In contrast to sex steroid receptors, which have highly conserved brain expression patterns across species, OXTR shows remarkable inter- and intra-species variation in brain distribution [2, 4]. For example, monogamous prairie voles have a brain OXTR distribution in cortex, striatum and amygdala that [4]is distinct from promiscuous montane voles and laboratory rats and mice. Furthermore, there is robust individual variation in brain OXTR expression among prairie voles that is associated with single nucleotide polymorphisms (SNPs) in the OXTR locus (*Oxtr*), and this variation predicts

pair bonding behavior and resilience to early life social neglect [5-8]. Different species of primates also differ in brain OXTR distribution [9], and SNPs in the human OXTR have been linked to variation in social function [10, 11]. Thus, variation in OXTR distribution in brain likely constitutes a mechanism for the emergence of diverse social traits, potentially including psychiatric endophenotypes.

Acute overexpression or knockdown of OXTR in a specific brain region alters social attachment and parental behaviors in monogamous prairie voles but not polygamous meadow voles [7, 12, 13]. A recent report showed that social attachment can occur in constitutive *Oxtr* knockout prairie voles [14], suggesting that developmental OXTR signaling may be essential for behavioral dependency on OXTR later in life. The direct cause-effect relationship between species-specific OXTR expression pattern and social behaviors, either developmentally or in adulthood, is unclear.

The evolution of gene expression patterns could be mediated by *cis* (via linked polymorphisms) or *trans* (through diffusible products of distal genes, e.g., transcription factors) changes, as a result of adaptation to the environment [15-17]. *Cis*-regulatory differences are more commonly responsible for adaptive evolution and interspecific divergence [18]. To explore the transcriptional mechanisms giving rise to species-specific *Oxtr* expression and social behavior, we created transgenic mice using a prairie vole *Oxtr* (pv*Oxtr*) bacterial artificial chromosome (BAC). The BAC construct covers the full coding sequence, introns and the entire intergenic region of the pv*Oxtr* with its neighboring genes. We expected two possible results: (1) our BAC construct accommodates all the critical promoter/enhancers elements responsible for species- and tissue-specific expression, therefore the *pvOxtr* transgenic mice would express brain *pvOxtr* in a prairie vole-like pattern; (2)The regulatory elements essential for species- and tissue-specific expression of *pvOxtr* in our BAC construct are not complete, the *pvOxtr* transgenic mice would express *pvOxtr* in a pattern different from either the prairie vole or the mouse. In either case, we can address our question: do developmentally distinct patterns of brain OXTR expression give rise to different social behaviors?

We obtained 8 lines of pv*Oxtr* mice with germline transmission, each "volized" (pv*Oxtr*) mouse line, i.e., each different integration site, displayed a unique pattern of expression in brain distinct from that of either wildtype mice or prairie voles. Intriguingly, *pvOxtr* expression was conserved in mammary gland across different lines. Moreover, different "volized" mouse lines showed differences in partner preference and maternal behaviors. These results demonstrate that transcriptional redistribution of brain OXTR in space and during development can support the emergence of variation in social preference and

parental behaviors, which natural selection could act upon and amplify in niches where the novel behavior is adaptive. In addition, our results provide important clues to understand the genetic mechanism underlying species differences in brain gene expression.

Results

Creation of the pv*Oxtr-P2A-Cre* BAC transgenic mice

BAC vectors can accommodate dispersed cis-regulatory elements across large regions of genome. Transgene expression from BAC constructs are generally resistant to insertion position effects [19] due to both the large spans of insulating genetic material which protect the transgene cassette from the influence of the chromosomal environment, and through the inclusion of necessary regulatory elements such as enhancers, silencers, locus control regions, and matrix attachment regions [20, 21]. Large-scale screening of CNS gene expression in BAC transgenic mice by the GENSAT (Gene Expression Nervous System Atlas) Project found that more than 85% of BACs express reproducibly in multiple independent transgenic lines and reporter gene expression faithfully recapitulates endogenous gene expression patterns [22-24]. Indeed, reproducible expression from mouse BAC vectors has been achieved for more than 500 genes [22-24]. Those that don't express reproducibly are influenced by variation in BAC copy number and insertion sites [25]. BAC engineering has also been used to mediate cross-species transgene expression. A large number of mouse models of human dominant neurodegenerative disorders have been created using human BAC transgene approaches. These model mice successfully express human transgenes in human-like patterns and recapitulate disease-like phenotypes [26-30]. We therefore decided to use BAC approaches to create "volized" *Oxtr* mouse lines.

The most important determinant for correct expression from BAC vectors is inclusion of as much of the intergenic region surrounding a gene of interest within the BAC construct as possible[25]. To create pv*Oxtr-P2A-Cre* BAC transgenic mouse line, we obtained a BAC clone (GeneBank: DP001214.1) from a prairie vole BAC library (CHORI-232) [31, 32] that includes the entire *pvOxtr* locus (the coding sequence and all the introns) with the full intergenic sequence upstream (150kb) and downstream of the *pvOxtr* coding region (9kb) (Fig1 B). The BAC clone contains a portion of *Rad18,* minus the first 11 exons, located upstream of *pvOxtr,* and *Cav3*, minus the first exon including the start codon, downstream of *pvOxtr.* Therefore, there will be no interference of these two flanking transgenes on behavior, and the proximal topological structure around *pvOxtr* locus is

preserved to the maximum extent. A P2A-NLS-Cre cassette was inserted in-frame just before the *Oxtr* stop codon to ensure co-expression of *Cre* and *Oxtr* (Fig1 C). Transgenic mice were generated by pronuclear injection using C57BL/6J zygotes. Proper integration of the reporter into the BAC clone was confirmed using gene specific PCR assays and sequencing (Fig1 C, D and data not shown). We obtained 11 founder mice carrying the transgenes, which was verified by PCR with multiple primer sets (Fig1 C, E). One founder line was sterile, and two founder lines did not show germ-line transmission. Eight founder lines successfully produced offspring and stably transmitted the transgene to at least 3 generations. We named these lines "Koi", meaning "love" in Japanese.

Each Koi line showed a unique expression pattern of transgene in brain, yet conserved expression in mammary gland.

We systemically evaluated 8 Koi lines by crossing them with ROSA-26-NLS-*LacZ* mice, a Cre reporter mouse line expressing nuclear-localized beta-galactosidase [33, 34]. Since Lac-Z is only expressed in the nucleus of double positive (CRE+, LacZ+) cells, but not in the neuronal processes, we could easily assess the expression pattern of our transgene. We found that each Koi founder line displayed a unique pattern of expression in brain distinct from that of wildtype mice or prairie voles (Fig2A-O, and supplementary Fig1). Almost all Koi lines showed transgene expression in olfactory bulb, lateral septum (Fig2F-I Supplementary Fig1B,E,H,K) and ventromedial nucleus of the hypothalamus (Fig2K-N Supplementary Fig1C,F,I,L), though with different intensities, suggesting that these regions constitute a stable core *Oxtr* expression network, as these regions also express OXTR in mice and voles [35, 36]. Several Koi lines expressed the transgene in some brain regions specific for vole *Oxtr* expression, including nucleus accumbens (NAc) (Fig2A,B,D Supplementary Fig1A,G,J), prefrontal cortex (PFC) (Fig2A,B,C Supplementary Fig1J), lateral amygdala (Fig2K,L,M Supplementary Fig1C,I,L) and deep layers of cingulate cortex (Fig2A,B,C Supplementary Fig1C,L), which suggested that cis regulatory elements in the BAC are capable of mediating the expression of *Oxtr* in the reward and reinforcement circuitry of brain, albeit depending on the sequence/structure of distal sequences >150 kb upstream and >21 kb downstream of the transcription start site. None of the Koi lines exactly "mirrored" the vole-specific expression patten. Six of the Koi lines expressed the transgene in broad areas of thalamus (Fig2K,L,N and Supplementary Fig1C,I,L), reminiscent of the strong expression of V1a vasopressin receptor (*Avpr1a*) in the thalamus [4]. Intriguingly, the expression of OXTR in mammary

glands showed similar pattern among all the Koi lines and *mouseOxtr(mOxtr)-Ires-Cre* knock-in line (Fig2P-T and Supplementary Fig2).

Transgenes that are introduced by pronuclear injection typically integrate into a single site of the genome as tandem concatemers [37]. BAC copy number variation and different insertional loci can lead to distinct patterns of ectopic expression, and increased BAC transgene copy numbers often correlate with increased BAC gene expression [25]. We then examined the relationship between transgene copy number and LacZ signal using quantitative genomic PCR [38]. As expected, the copy number of WT, heterozygous and homozygous *mOxtr-Ires-Cre* knock-in mice was 0, 1 and 2 respectively (Figure2Z). The copy number of transgene in Koi lines are: Koi-1 (12), Koi-2 (2), Koi-3 (2), Koi-4 (1), Koi-5 (2), Koi-6 (4), Koi-7 (9), Koi-8 (3). Koi-6 and Koi-7 showed the most limited expression of reporter gene, though the copy number of transgene were 4 and 9 respectively. Koi-4 showed strong expression of reporter gene in NAc, septum and thalamus, though there was only 1 copy of transgene. Therefore, integration site rather than copy number is the reason of the variant BAC transgene expression patterns across our Koi lines.

Oxtr is localized to a boundary of large Topologically Associating Domains

The divergent brain expression patterns across our Koi lines suggest that distal elements external to our BAC cassette may contribute to the variation in *Oxtr* expression. Topologically associating domains (TADs) represent a key feature of hierarchical genome organization comprising chromatin regions that frequently interact within the chromatin domain while insulating regulatory interactions across TAD boundaries [39-42]. Hi-C assays provide a genome-wide view of chromosome conformation in multiple layers, including TADs [43, 44]. Utilizing publicly available 3D chromatin datasets from mouse (Supplementary Table1), we discovered that *Oxtr* is consistently located at the boundary region of TAD structures (approximately 2000kb) across several tissues and cell lines (Supplementary Fig3A). Specifically, only in brain related samples (whole brain tissue, neural progenitor cells, and cortex tissue), *Oxtr* is situated at the boundary of a large inter-TAD interaction between two neighboring TADs, forming larger TAD structures (approximately 4000kb) (Supplementary Fig3A). In contrast, the oxytocin peptide gene, *Oxt*, which is expressed in a highly conserved brain pattern across vertebrates, lacks such organized large TAD structures (Supplementary Fig3B). Analysis with the datasets from human brain-related samples revealed that human *Oxtr* is also localized at the boundary region of TAD structures, though the heatmap showed a clearly distinct pattern with that

of the mouse (Supplementary Table2; Supplementary Fig4A). Like in mouse, human *Oxt* doesn't show typical TAD structures (Supplementary Fig4 B). Although the Hi-C data was not generated from prairie vole tissues, it demonstrates that the TAD landscape is dramatically different between *Oxtr* and *Oxt* and highlights that the 3D genomic structure surrounding the *Oxtr* gene varies across species and tissues.

Adult brain OXTR binding patterns differ across Koi lines

To detect the distribution of OXTR protein in adult Koi lines without the interference of endogenous mouse OXTR (mOXTR) signal, Koi lines were crossed with *mOxtr*$^{-/-}$ mice and pvOXTR binding was detected using receptor autoradiography. We focused on 4 Koi lines: Koi-1, Koi-2, Koi-3 and Koi-4 based on the strong expression of reporter gene in behaviorally relevant neuronal populations. Autoradiography demonstrated functional pvOXTR in brain resembling to some extent Cre-induced reporter gene expression (Figure 3). Brain OXTR binding of Koi-3 was consistent with Lac-Z expression in the reporter line (Fig2C, H, M and Figure3 J-L). Interestingly, the OXTR binding in PFC of Koi-3 was similar to that of prairie vole. In contrast, Koi-4 showed low OXTR binding in NAc when compared with the high Lac-Z staining (Fig2D, Figure3M), consistent with transient *pvOxtr* expression during development, a pattern previously reported in rat NAc [45]. Cre-dependent reporter gene product reflects the cumulative expression history of the transgene throughout development. Koi-2, the line which displayed the expression of reporter genes in the broadest regions, did not show strong signal in autoradiography, again suggesting developmental changes in transgene expression. It is interesting that Layer IV of cortex in Koi-4 showed strong OXTR binding (Figure3 N and O), which is highly likely to originate from the axon projections from the thalamus (Fig2N), as was previously reported for NAc projections in voles [46]. Consistent with Lac-Z expression, we do not see a clear relationship between OXTR binding and transgene copy number. For example, Koi-1 showed low OXTR signal (Fig3 D, E, F) with the highest copy number, while Koi-4 showed very strong OXTR signal at lateral septum and thalamus (Fig3 N, O), with the lowest copy number. *Oxtr* expression level was further confirmed with qRT-PCR (Supplementary Fig 5, 6). Though OXTR binding in NAc of Koi-4 was barely detected using autoradiography, the more sensitive qRT-PCR revealed that adult Koi-4 mice had the highest Oxtr mRNA signal in the striatum, several fold higher than WT, consistent with the Lac-Z staining in the reporter line.

Although none of our Koi lines mirrored the endogenous OXTR expression in prairie voles, we confirmed strong expression of *pvOxtr* in olfactory bulb of Koi-1line, PFC and

amygdala of Koi-3line, striatum and thalamus of Koi-4 lines, and the broad expression of *pvOxtr* in Koi-2 line. As OXTR signaling in some of these regions are similar to that in voles, albeit in separate lines, and postulated to be involved in vole social behavior [47], we used these lines to address the question of whether developmental variation in *Oxtr* transcription in brain can lead to variation in social behaviors.

Different Koi lines showed diverse behaviors in a Partner Preference Test

The partner preference test is widely used as a laboratory proxy for pair bonding in prairie voles. In a pilot study, we found that Kio-4 female mice on a m$Oxt^{+/+}$ background showed a preference for their mate relative to a novel male. We then focused on the females of 4 lines (Koi-1, 2, 3, 4) based on transgene expression in PFC, BLA or NAc. We bred the transgenic mice with $mOxtr^{-/-}$ mice (both on C57/B6 background) to generate offspring expressing only pv*Oxtr*. Partner preference tests (PPT) were performed in ovariectomized females after 21 days of cohabitation with 3 mating bouts elicited by estrogen and progesterone injections on days 2, 9 and 16. We divided our analysis into 3 phases (Fig4A, B). In the habituation phase, the experimental subject was habituated to the chamber for 5 minutes with both pen-boxes empty. In the recognition phase, the partner stimulus animal was restricted in one pen-box, and a novel “stranger” male was restricted in another pen-box, and the experimental female was allowed to explore the arena for 10 minutes to test social novelty preference. In the preference phase, the positions of the partner stimulus animal and the “stranger” stimulus animal were switched to avoid position bias, and the female was allowed to explore the chamber for an additional 20 minutes.

Mixed ANOVA was conducted to examine the effect of genotype and the stimulus box on the area stay time during all the phases. In the habituation phase (Fig4C), there was no statistically significant interaction between the effects of genotype and position of empty pen-box on stay time, $F(4, 60) = 0.69$, $p = 0.6$. There was no difference in position preference for all the groups, $F(1,60) = 0.03$, $p = 0.87$. In the recognition phase (Fig4D), there was a main effect of stimulus animal (i.e., partner or stranger) on stay time, the time staying in close proximity to the partner was significantly shorter than the time stay with stranger animal ($F(1,60) = 15.38$, $p < 0.001$). There was a main effect of genotype on social stay time, $F(4,60) = 2.62$, $p < 0.05$, and a significant interaction between the effects of genotype and stimulus animal on area stay time, $F(4, 60) = 2.61$, $p < 0.05$. Bonferroni adjusted pairwise comparisons were applied to analyze the simple main effects. Koi-4 and WT mice spent significantly longer time in "stranger" area than in "partner" area ($p<0.05$),

demonstrating a typical novelty preference. There was no significant difference between the stay time with "stranger" and "partner" for Koi-1 ($p=0.96$), Koi-2 ($p=0.49$) and Koi-3 ($p=0.09$) mice. In the preference phase (Fig5E), conducted after both stimulus mice were presumably familiar following the initial 10 min recognition phase, there was no main effect of stimulus animal on stay time, $F(1,60)=0.04$, $p=0.84$. There was no main effect of genotype on stay time either, $F(4,60)=1.36$, $p=0.26$. There was a statistically significant interaction between the effects of genotype and stimulus animal on area stay time, $F(4, 60) = 4.64$, $p<0.01$. Bonferroni adjusted pairwise comparisons revealed that Koi-2 mice spent significantly longer time in "stranger" area than in "partner" area ($p<0.05$). In contrast, Koi-4 mice spent significantly longer time in "partner" area than in "stranger" area ($p<0.01$). There was no significant difference between the stay time with "stranger" and "partner" for WT ($p=0.99$), Koi-1 $p=0.16$) or Koi-3 ($p=0.45$) mice.

Different Koi lines showed diverse behaviors in Pup Retrieval Test

Based on the abundant pvOXTR of Koi-3 and Koi-4 in reward-related brain regions (Fig3J-O), and the role of OXTR in mediated maternal care in mice and voles [48-50], we further tested the parental behaviors of these two lines in virgins (Fig4F, G). Mixed ANOVA was conducted to examine the effect of genotype and pup number (1-3) on the latency of pup retrieval. Mauchly's test showed that the sphericity was violated. Therefore, the Greenhouse-Geisser correction was used for the repeated measures ANOVA. There was a significant main effect of genotype on latency to retrieve, $F(2,48)=29.58$, $p<0.0001$. Koi-4 took a significantly longer time to retrieve all the pups than WT and Koi-3 ($p<0.0001$ for both). There was also a significant interaction between the effects of genotype and retrieved pup number on the retrieval latency, $F(2.40, 57.49) = 4.45$, $p<0.05$. Post Hoc multiple comparisons with Bonferroni correction revealed that Koi-4 took a significantly longer time to accomplish the 1st retrieval ($p<0.001$), the 2nd retrieval ($p<0.0001$), and the 3rd retrieval ($p<0.0001$) when compare to WT and Koi-3. And Koi-3 took a significantly shorter time to accomplish the 1st retrieval ($p<0.05$), the 2nd retrieval ($p<0.01$), and the 3rd retrieval ($p<0.01$) when compare to WT.

Crouching time was analyzed as well (Fig4F, H). There was a statistically significant difference between groups as determined by one-way ANOVA ($F(2,48) = 27.56$, $p<0.0001$). A Bonferroni post hoc test revealed that the crouching time of Koi-3 was statistically significantly longer than WT ($p<0.01$) and Koi-4($p<0.0001$). Additionally, the crouching time of Koi-4 was statistically significantly shorter than WT ($p<0.01$).

Therefore, two Koi lines with different OXTR expression pattern demonstrated quantitative differences in parental behavior tests.

Discussion

Diversity of developmental *Oxtr* expression patterns causes diversity of social behaviors

The diverse OXTR expression of our Koi lines is reminiscent of the diverse OXTR expression across different species. Species and individual differences in OXTR distribution in the brain have been associated with variation in social behaviors [2, 4]. For instance, the monogamous prairie vole expresses high densities of *Oxtr* in the PFC, NAc and BLA compared to non-monogamous vole species or mice. Pharmacological and viral mediated siRNA manipulations of OXTR in adult vole PFC and NAc suggest that OXTR in these regions play a role in parental care and pair bonding[12, 13, 48]. Furthermore, variation in prairie vole OXTR expression in brain are also associated with individual differences in parental behavior, pair bonding, and resilience to neonatal neglect[5, 8, 51, 52]. However, it is unclear whether inter- or intra-species variation in brain OXTR signaling during development, due to variation in brain expression pattern, is causally mediating diversity in social behaviors. We obtained expression in PFC, NAc and BLA regions in our Koi mice, but in 3 separate lines. These Koi lines with distinct brain OXTR expression pattern provided an opportunity to test the causal effect of development variation of OXTR expression on diverse social behaviors developmentally.

In contrast to wildtype mice, the Koi-4 line showed a preference for their mating partners over unfamiliar males, as is typically observed in prairie voles. Multiple studies showed that NAc and PFC play important roles in mediating partner preference behavior in prairie voles [53, 54]. Although the Koi-4 line showed robust transgene expressed in these regions using the Lac-Z reporter mouse method, qPCR and receptor autoradiography suggest more limited OXTR expression as adults, albeit several fold higher than WT mice, suggesting transient changes in transgene expression during development. Emerging research have shown that species differences exist in developmental patterns of OXTR expression. For example, pre-weaning rats have a transient peak OXTR specifically in NAc and cingulate cortex [55, 56], while mice have a transient peak of OXTR throughout the entire neocortex [57]. Transient OXTR expression may define sensitive periods for oxytocin to shape the brain development of those brain regions in a social stimulus dependent way[58]. OXTR signaling in the NAc during the first two weeks of life appear to shape adult partner preference behavior in prairie voles [5]. The brain regions that display transient appearance of OXTR are not

conserved across species, and transient OXTR expression may help to shape activity-dependent development and contribute to adult social behaviors in a species-specific manner [59]. Partner preference formation and maintenance needs to recruit multi- and cross-modality sensation, social recognition and social memory, selective attention, arousal, and reward systems. We propose a model that the sufficient upregulation of the OXTR expression in one or multiple of these systems can tune the network and boost partner preference behavior. In addition, the maternal behavior in Koi-3 and Koi-4 lines was enhanced and reduced, respectively. This result suggested that OXTR signaling facilitates social partner preference and maternal care by coordinating activity across different neural networks. A main conclusion of our study is that simply by redistributing OXTR binding in space and during development, variation in social preference and parental behaviors emerged, which conceivably could impart advantageous behaviors that natural selection could act upon and amplify. Future study will determine how the variation in OXTR distribution in our Koi lines affects neural circuits mediating social behaviors.

A potential genetic mechanism contributing to diversity of brain OXTR expression and social behavior

The sex steroid and oxytocin systems play important roles in modulating reproductive and related social behaviors in vertebrates. Sexual behavior, e.g., the motivation to mate and motor patterns, is highly conserved across vertebrate species. By contrast, social behaviors, e.g., sociality, mating strategy (monogamy vs polygamy), parental and alloparental behaviors are more nuanced and can vary dramatically across species in the same genus or even between individuals of a single species. It is interesting, therefore, that the distribution of steroid receptors is quite conserved among species [60], while that of the OXTR is extremely diverse across and even within species [2, 4]. It is even more interesting that although the distribution of OXTR is diverse, its ligand, oxytocin, is expressed in a highly conserved neuroanatomical pattern in vertebrates [61]. Previous work showed that three independent rat lines with puffer fish oxytocin BAC transgene (containing 16 kb of 5' flanking regulatory sequence) expressed the *Fugu* oxytocin transcript specifically in oxytocin neurons in rat [62]. Moreover, a similar transgenic experiment transferring approximately 5 kb of the *Fugu* oxytocin already resulted in a faithful expression of the fish genes in mouse oxytocin neurons [63]. These studies suggest there is a remarkably conserved transcriptional regulatory machinery across species, even between the *Fugu* and rodent oxytocin genes, despite being separated by

400 million years of evolution. Finally, 2.6 kb of the oxytocin promoter is sufficient to faithfully express transgenes in oxytocin neurons when delivered using a viral vector[64].

Based on the principle of choosing a proper BAC clone to create BAC transgenic mice, the most important determinant for correct expression from BAC vectors is inclusion of as much as possible of the 5' and 3' intergenic region surrounding a gene of interest [23, 25, 65]. The *pvOxtr* BAC clone we chose carries the entire *pvOxtr* locus with the full intergenic sequence upstream and downstream of *pvOxtr*. Though in some cases BAC sequences don't include the whole TAD, they still contain the critical tissue-specific control elements for the locus, and can confer reproducible, accurate expression patterns of transgenes [66]. However, the 8 lines we obtained demonstrated remarkably variant brain pvOXTR expression, distinct from both prairie vole and mouse. The different expression pattern is not from the copy number of transgenes. Instead, it is most likely due to the effects from different insertion sites of transgenes. These results are reminiscent to the observation that virtually every rodent or primate species examined has a unique distribution of OXTR binding in the brain. Our 3D genomic structure analysis using open databases showed that the mouse *Oxtr* and human *OXTR* loci sit within large TAD structures, while no typical TAD structure surrounds *Oxt* loci in either species. Considering the size of TADs where *Oxtr* locates in brain related tissues both in mouse and human (about 4000kb), certain regulatory elements (including insulator sequences) essential for brain-specific expression of *pvOxtr* may lie outside of the BAC region. This might explain why short promoter sequences suffice for faithful expression of oxytocin across species and when employing viral vectors, but a 200kb BAC is not adequate for precise, reproducible transcription regulation of *Oxtr*. This may also account for the transcriptional hypersensitivity of *pvOxtr* to chromosomal position effect in brain.

It is also noteworthy that pv*Oxtr* expression in mammary gland were conserved across different Koi lines. These results suggested that the promoter/enhancer/insulator elements critical for mammary gland-specific expression of *pvOxtr* are encompassed by the BAC construct, and the regulation of *pvOxtr* expression in mammary gland is highly resistant to the position effect of integration sites. Our 3D genomic structure analysis using mouse datasets showed that the chromatin landscape differs considerably between brain-related tissues and other tissues. This is observed by an obvious increase of long-distance interactions between neighboring TADs, forming a larger TAD structure in brain-related tissues. We here propose a new genetic model of *Oxtr* expression regulatory machinery: The sequence proximal to *Oxtr* loci within the BAC construct is sufficient to form a complete regulatory unit. This unit is resistant to changes in interactions with distal

regulatory sequences and confer faithful expression of OXTR in peripheral tissues where OXTR expression is essential for reproduction. In contrast, interacting regulatory elements that govern brain region-specific expression of OXTR are dispersed over a large sequence, extending far beyond the BAC construct. This makes OXTR expression in brain susceptible to the chromosomal landscape, even at locations very distal to the gene loci. This is well aligned with the notion that subtle changes in 3D chromatin structure may result in substantial changes in local gene expression [67]. Such an organization could offer increased opportunities for chromosomal variation across species to impart evolvability (the capacity of an evolving system to generate or facilitate adaptive change) of *Oxtr* expression in the brain. Consequently, this would allow oxytocin to modulate novel neural circuits, which can then modify various facets of social behavior, leading to the evolution of diversity in social behaviors. If the resultant behavior is adaptive, the frequency of the mutation will increase in the population and the social behavioral profile of the population may change. Future work applying Hi-C and ChIP approaches on different brain regions and peripheral tissues from prairie vole, montane vole and our Koi lines to see the chromatin structure and epigenetic landscape surrounding *Oxtr*, will be very helpful to understand how TAD landscape and epigenetics influences *Oxtr* gene expression and social behavior traits.

There is other experimental evidence supporting the notion that brain expression of *Oxtr* is labile, sensitive to genetic variation. SNPs in the *Oxtr* intron explains 74% of the variance in striatal *Oxtr* expression and social attachment in prairie voles [8] and it is possible that these SNPs near *Oxtr* are linked to larger distal variations that affect brain *Oxtr* expression. Different *Oxtr*-reporter (either lac-z, EGFP or Venus etc.,) mice created from independent labs either by knock-in or BAC transgene methods showed different expression pattern in brain as well [25, 35, 65], further supporting the ultra-sensitivity and lability of *Oxtr* gene to subtle changes of distal cis sequence and local chromosomal architecture. Additionally, SNPs in the human OXTR predict OXTR transcripts in a brain regions-specific manner [68] as well as brain functional connectivity[69]. This transcriptional ultra-sensitivity to genomic variation appears to be tissue specific and mainly appears in brain, but not in mammary gland, which is responsible for essential lactation in mammals.

Another interesting point is that *Oxtr* is localized at TAD boundary regions in mouse and human. TAD boundaries are thought to be essential for normal genome function, given their roles in defining regulatory territories along chromosomes and in preventing

unintended enhancer-promoter interactions between adjacent chromatin domains. Cross-species multiple sequence alignments have revealed an enrichment of syntenic breaks at TAD boundaries[70]. Future studies will explore synteny regions along the *Oxtr* TAD in different species.

In summary, we created mouse lines showing different expression pattern of brain OXTR using a BAC transgenic method. Our results suggest that complex, long-distance interactions between proximal and distal cis regulatory elements contribute to region-specific expression in brain, but not mammary tissue. The variability in transgene expression pattern in brain depending on integration site suggest that *Oxtr* expression is sensitive to large-scale chromosomal interactions, which may impart evolvability of *Oxtr* expression patterns in the brain. Subtle variation in chromatin landscape of *Oxtr* gene may alter long distance regulatory interactions, and thereby alter brain expression patterns and lead to the emergence of novel social behaviors, which may allow organisms to adapt to and survive variable environments. We speculate that this transcriptional evolvability may contribute to inter- and intra-specific *Oxtr* expression patterns in brain. We also confirmed for the first time the causal effect of developmental variation in brain *Oxtr* distribution on the diversity of social behaviors. Our mice lines with different Oxtr expression patterns display differences in partner preference and enhanced or reduced parental behaviors. This research on the origins of diversity in social behaviors across species may lead to conceptual understandings relevant for the development of treatments for psychiatric disorders.

Acknowledgements:

This work was supported by the International Education and Research Laboratory Program of University of Tsukuba to L.Y., the RIKEN Incentive Research Project (100226201701100443) to Q.Z., the Brain Science Project, Center for novel science initiatives, National institutes of natural sciences (BS291003) to Q.Z., the RIKEN Aging Project (10026-201701100263-340120) to Q.Z., the JSPS Kakenhi Grant-in-Aid for Young Scientists (17K18362) to Q.Z., the JSPS Kakenhi Grant-in-Aid for Challenging Research (19K21807) to Q.Z., the JSPS Kakenhi Grant-in-Aid for Challenging Research (2 2 K 1 9 4 7 8)to Q.Z., and the Takeda Medical Research Grant to Q.Z.. We thank Dr. Katsuhiko Nishimori (Tohoku University and Fukushima Medical University, Japan) for providing *mOxtr-Ires-Cre* knock-in line and *mOxtr*$^{-/-}$ mutant line; Dr. Cary Lai (Indiana University, USA), Dr. Takuji Iwasato(National Institute of Genetics, Japan) and Dr. Seiya

Mizuno(University of Tsukuba, Japan) for their advice on BAC vector construction; Dr. Volkhard Maeckel (CERN, Switzerland) for helping with image capturing; Dr. Yong Zhang (Tongji University, China) for the stimulating discussion about 3D chromatin structure, and we thank the Laboratory of Animal Resource Center of University of Tsukuba for pronuclear injection.

Author Contributions:

Q.Z. conceived the project, designed the study, led the teamwork, conducted transgene vector construction and drafted manuscript. Q.Z. and L.N. and K.N analyzed Hi-C datasets. Q.Z., L.K. and M.T. conducted histological analysis. Q.Z. and M.P. analyzed transgene copy number and gene expression level. Q.Z. and K.I. conducted autoradiography analysis. Q.Z., L.K., M.T. and M.P. performed behavioral test and analyzed the data. Y.N. and T.S. performed ovariectomy surgery. L.K., M.T., M.S. and M.P. performed genotyping and mouse maintenance. S.I. provided advice and facility for transgene vector construction. L.Y helped conceive the project, provided advice for the whole project and edited the manuscript. All authors discussed the manuscript.

Declaration of Interests:

The authors declare no competing interests.

Figure titles and Legends:

Fig.1 Construction of Koi lines. (A) Example of the remarkable species difference of brain OXTR distribution. OXTR receptor autoradiography in dorsal caudate putamen (CP) and nucleus accumbens shell (NAccSh) of rat, mouse, and prairie voleis (Adapted Froemke and Young[2]). (B) The *pvOxtr* BAC clone contains the entire sequence of *pvOxtr* gene (colored green), the complete intergenic sequence both upstream and downstream of *pvOxtr* gene, the 12th exon of *Rad18* (colored blue) and the 2nd exon of *Cav3* (colored purple). The yellow arrows indicate the direction of transcription. (C) Schematic diagram of the strategy to generate Koi mice. The P2A-NLS-Cre-Frt-Amp-Frt cassette was inserted in-frame right before the stop codon of *Oxtr*. And the ampicillin selection marker was deleted by 706-Flpe. PCR primers for verifying the targeted alleles are shown as red arrows. (D) Two correctly modified vector clones were verified by using PCR with p2 and p8. (E) Koi lines were verified by 5 pairs of primers. From Lane1 to Lane8 are 100bp marker, p3+p7, p2+p6, p2+p7, p4+p8, p2+p8, blank and 1kb marker.

Fig.2 Transgenic CRE mediated Lac-Z reporter gene expression in the brain and mammary gland of Koi lines. X-gal staining of the brains and mammary glands are from the double positive (*Cre*+, *LacZ*+) offspring from Koi-1 (A, F, K, P), Koi-2 (B, G, L, Q), Koi-3 (G, H, M, R), Koi-4 (D, I, N, S) and *mOxtr-Ires-Cre* knock-in line (E, J, O, T). U, V, M, X, Y are the magnified images of the areas within the yellow-border squares from D, N, E, J, O, respectively, to show the distribution of low-density Lac-Z positive cells in these areas. Scale bar=1mm (A-O), 500um (P-T) and 200um (U-Y). (Z) The estimated copy number of transgene of all Koi lines. See Supplementary Figure 2 for images of Koi-5-8 lines. PFC=prefrontal cortex, LS=lateral septum, BLA=basolateral amgydala, VMH=ventromedial nucleus of the hypothalamus, Tha=thalamus.

Fig.3 The expression of OXTR in adult brain of Koi lines. Autoradiographs illustrate the distribution of OXTR binding in adult WT (A-C), Koi-1 (D-F), Koi-2 (G-I), Koi-3 (J-L), and Koi-4 (M-O). PFC=prefrontal cortex, LS=lateral septum, BLA=basolateral amgydala, VMH=ventromedial nucleus of the hypothalamus, Tha=thalamus. Scale bar=1mm.

Fig.4 Social behaviors of Koi lines. (A) Illustration of the partner preference test (PPT) paradigm. The experimental mouse was placed in a chamber with an automatic monitoring system, where it could freely explore two pen-boxes localized in two diagonal corners. Habituation phase: two pen-boxes are empty. Recognition phase: a stimulating partner mouse is placed into one pen-box and a stimulating stranger mouse is placed in the other one. Preference phase: The positions of two stimulating mice are switched. (B) Representative traces of one experimental mouse during the three phases. (C-E) The stay time in the surrounding area of each pen box during three phases;(C) Habituation phase;(D) Recognition phase; (E) Preference phase. Samples sizes for the PPT are WT (n=12), Koi-1 (n=14), Koi-2 (n=13) Koi-3 (n=12) Koi-4 (n=14). All the experimental mice are female. (F) The illustration of the procedure of the maternal behavior test. (G) Pup retrieval latency and (H) crouching time were recorded and analyzed. Sample sizes for the maternal behavior tests are WT (n=15), Koi-3 (n=18), Koi-4 (n=18). Significance of interaction between independent factors: # $p<0.05$; # # $p<0.01$. Significance of main effect or single main effect of genotype: * $p<0.05$; * * $p<0.01$; * * * $p<0.001$; * * * * $p<0.0001$.(Illustrations created with Biorender.com)

Star Methods

***pvOxtr-P2A-Cre* BAC vector construction**.

The vole BAC clone (GeneBank: DP001214.1) containing the *Oxtr* locus was obtained from a prairie vole BAC library (CHORI-232) [31, 32]. This BAC clone carries the entire *pvOxtr* locus with the full intergenic sequence upstream of 5' of *pvOxtr* (150kb) and downstream of coding region of *pvOxtr* (9kb). The NLS (nuclear localization signal)-Cre-Frt-Amp-Frt cassette was obtained from Dr. Takuji Iwasato, and was slightly modified to introduce a P2A sequence [71]. The P2A sequence was introduced using PCR with the following primers:

fw5'- ATGGGAAGCGGAGCTACTAACTTCAGCCTGCTGAAGCAGGCTGGAGA

CGTGGAGGAGAACCCTGGACCTCTCGAAACTGACAGGAGAACCACC-3';

rv5'-AGACTGGAGTCCGCATAGCCCCCCTCCCCCGCCCCAGGCGCGGTGGGCC

AGGCAGGTGGCTCACCTTGACCAAGTTGCTGAAGTTCCTATTCC-3'. The P2A sequence is underlined. And the resulting amplified cassette had the P2A upstream of the NLS-Cre. Then the P2A-NLS-Cre-Frt-Amp-Frt cassette was inserted in-frame right before the stop codon of Oxtr in the BAC clone using the Red/ET Recombineering kit (Gene Bridges GmbH, Heidelberg Germany) after adding homologous arms by PCR with the following primers: fw5'-CACCTTCGTCCTGAGTCGCCGCAGCTCCAGCCAGAGGAGCTG

CTCTCAACCATCTTCAGCAATGGGAAGCGGAGCTACTAAC-3';

rv5'-GAGGAGAGGGATACACACCAATAGGCACCTTATACAACTCCACGCAC

GGCCACCAGGGGCAGACTGGAGTCCGCATAGCC-3'. The ampicillin selection marker was deleted with the 706-Flpe-induced recombination method (Gene Bridges Heidelberg Germany). A correctly modified BAC clone was verified by using PCR at both the 5' and 3' junctions of the targeted insertion with the following primer pair : fr5'-GCCTTCATCATCGCCATGCTCTT-3'(p2) and rv5'-GATGGCTGAGTG ACTGGCATCT-3'(p8); The construct was further verified by sequencing using the following 7 primers specific either for BAC vector or the p2A-NLS-Cre fragment:

5'- CCTGCAGCCAACTGGAGCTTC-3'(p1); 5'- CTTCCTTGGGCGCATTGACGTC-3'(p5); 5'-TACCTGTTTTGCCGGGTCAG-3(p4) ; 5'-GCCTTCATCATCGCCATGCTCTT-3'(p2) ; 5'-CTGACCCGGCAAAACAGGTA-3'(p7) ; 5'-TCCGGTTATTCAACTTGCACCATGC-3'(p6); 5'-GATGGCTGAGTGACTGGCATCT-3'(p8).

Animals.

***pvOxtr-P2A-Cre* BAC transgenic mouse lines (Koi lines)**. *pvOxtr-P2A-Cre* BAC vector was digested with NotI for linearization and to remove the pTARBAC vector backbone. The *Vole-Oxtr-P2A-Cre* BAC linearized fragment was purified using CL-4B sepharose

(Sigma-Aldrich), and injected into pronuclei of C57BL/6J zygotes. Mice carrying the BAC transgene were identified and confirmed using PCR with 5 pairs of primers: fr5'-TCGACCAGGTTCGTTCACTC-3'(p3) + p7; p2+ p6; p2 +p7; p4 +p8; p2+p8. 8 lines (Koi-1~Koi-8) were confirmed with successful transgene inheritance. These lines were maintained on a congenic C57BL/6J background by backcrossing with wildtype C57BL/6J for assessments of BAC DNA copy numbers and initial transgene expression analysis. The ***ROSA-26-NLS-LacZ*** **mouse** line [33] was obtained from Itohara Lab at RIKEN. The ***mOxtr-Ires-Cre*** **knock-in** [72] and ***mOxtr*$^{-/-}$ mutant** [73] lines were obtained from Dr. Katsuhiko Nishimori at Tohoku University, and both were backcrossed with C57BL/6J for more than 10 generations. Each Koi line and *mOxtr-Ires-Cre* knock-in mice were crossed with *ROSA-26-NLS-LacZ* mice to generate Cre^{+}, $LacZ^{+}$ double positive mice for further gene expression analysis. Koi mice were then crossed with *Oxtr*$^{-/-}$ to generate mice in which the pvOXTR was expressed while endogenous mOXTR was absent, and these mice were used for autoradiography, qRT-PCR and behavioral tests. All mice were generated using continuously housed breeder pairs and P21 as the standard weaning date. All the animal procedures were approved by University of Tsukuba Animal Care and Use Committee. Mice were housed under constant temperature and light condition (12 h light and 12 h dark cycle), and received food and water ad libitum.

Determination of transgene copy number

Custom Taqman® MGB probes were synthesized by oligoJp (Thermo Fisher, Japan) for detecting the transgenic *Cre* and the mouse *Jun* gene (internal control). The following primer pairs and probes were used: for the *Cre* assay, fr5'-ATGACTGGGCACAACAGACAAT-3'; rv5'- CGCTGACAGCCGGAACAC-3'; probe: 5'-FAM- AAACATGCTTCATCGTCGGTC CGG-MGB-3'; for *Jun* assay, fr5'-GAGTGCTAGCGGAGTCTTAACC-3'; rv5'-CTCCAGACGGCAGTGCTT-3'; probe: 5'-VIC-CTGAGCCCTCCTCCCC-MGB-3'. Real-time PCR was performed using an Applied Biosystem7500. Transgene copy number was determined through absolute quantification (standard curve method) following the protocol described in [38]. Briefly, 2 microliters (20 ng) of genomic DNA samples or copy number standards were analyzed in a 20μL reaction volume with two primer-probe sets (*Cre, Jun*). The data from transgenic samples were then compared to a standard curve of calibrator samples that are generated by diluting purified BAC DNA (linearized) over a range of known concentrations into wild-type mouse genomic DNA. In addition, no-template controls were included in each experiment. All reactions were performed in triplicate.

626

627 **Histology**

628 Adult mice (3-4month old), 4 male and 4 female from each line/ generation were
629 analyzed for 3 generations. Mice were perfused intracardially with 4% formalin in 0.1M
630 sodium phosphate buffer. Brains were embedded in 2% agarose in 0.1M PB and cut into
631 100-m-thick sections with a Micro-slicer (Dosaka, Kyoto, Japan). Mammary glands were
632 isolated from virgin female mice (2month old), 2 mice/each line were analyzed. The brain
633 slices and whole mount mammary glands preparation were stained in X-gal solution (5
634 mM K3FeCN6, 5mMK4FeCN6,2mMMgCl2, 0.02% NP-40, 0.01% Na-deoxycholate, 1
635 mg/ml X-gal in 0.1M PB) at 37°C for 6 hours and then were stained with hematoxylin.
636 All experiments were done with positive and negative controls (Cre^+, $LacZ^-$) to monitor
637 the reliability of the X-gal staining. Images were caught by Nanozoomer 2.0-HT slide
638 scanner (Hamamatsu Photonics).

639

640 **3D chromatin verification on Hi-C datasets of humans and mice**

641 The 3D genome structure tracks were obtained from 4DNucleome Consortium
642 (https://www.4dnucleome.org/) where datasets were systematically reanalyzed following
643 recommended standard protocols. The datasets IDs and sample information are provided
644 in the supplementary material (Supplementary Table1,2). 3D Genome Browser[74] and
645 WashU Epigenome Browser[75] were employed for visualizations.

646

647 **Receptor Autoradiography**

648 OXTR autoradiography was performed as previously described [36]. Briefly, freshly
649 frozen brains were stored at -80˚C. Coronal sections were cut in a cryostat and 20 µm
650 sections were collected and then stored at -80˚C until use in autoradiography. Brain
651 sections were removed from -80˚C storage and air dried, and then fixed for two minutes
652 with 0.1% paraformaldehyde in PBS at room temperature, and rinsed twice in 50
653 mM Tris buffer, pH 7.4, to remove endogenous OT. They were then incubated in 50 pM
654 125I-OVTA (2200 Ci/mmol; PerkinElmer; Boston, MA), a selective, radiolabeled OXTR
655 ligand, for one hour. Unbound 125I-OVTA was then washed away with Tris-$MgCl_2$
656 buffer (50 mM Tris plus 2% MgCl2, pH 7.4) and sections were air dried. Sections were
657 exposed to BioMax MR film (Kodak; Rochester, New York) for five days. Digital images
658 were obtained with a light box and a Cannon camera (Cannon 6D MarkII, Japan). The
659 brightness and contrast of representative images were equally adjusted for all
660 autoradiography images within a panel using Adobe Photoshop.

Quantification of *Oxtr* mRNA expression by qRT-PCR

Real-time quantitative polymerase chain reaction (RT-qPCR) using an Applied Biosystems 7500 Real-Time PCR system was used to quantify *Oxtr* mRNA expression levels in different brain regions of Koi lines. Total RNA of different brain regions was isolated using the RNeasy extraction kit (Qiagen, Germantown, US), and cDNA was synthesized after Deoxyribonuclease I (Invitrogen, Waltham, US) treatment by using EvoScript Universal cDNA Master (Roche, Penzberg, Germany), and then quantitative RT-PCR was performed with FastStart Universal SYBR Green Master (Roche, Penzberg, Germany). The relative standard curve method was used to obtain the relative quantities of *Oxtr* expression following the manual of Applied Biosystems. To allow the comparation between Koi lines and WT mice, the following primer pair (which can detect the expression of both *mOxtr* and *pvOxtr*) was used: fr5'-GCCTTTCTTCTTCGTGCAGATG-3' and rv5′-ATGTAGATCCAGGGGTTGCAG-3′ In addition, to specifically detect the expression of *pvOxtr*, the primer pair fr5′-GCCTTTCTTCTTCGTGCAGATG-3 and rv5'-AAAGAGGTGGCCCGTGAAC-3′ was used in the 2nd qRT-PCR experiment. GAPDH was used as the endogenous control for both experiments and was amplified by the following primer pair: fr5'-GGGTTCCTATAAATACGGACTGC-3' and rv5'- CCATTTTGTCTACGGGACGA-3'. Samples were analyzed in triplicates. A non-template control was performed to ensure that there was no amplification of genomic DNA. All of the experimenters were blind to the genotype of the subjects.

Partner preference test (PPT)

Subjects were housed with 4 age-matched and same-sex littermates until testing at adulthood (2-5 months old). 12-14 homozygous? mice were tested for each group. Ovariectomized females were paired and cohoused with a sexually experienced adult wildtype male for 21 days before PPT test. The female was injected with estradiol benzoate (10 μg and 5 μg at 48 h and 24 h before induced mating) and progesterone (500 μg at 4–7 h before induced mating) to ensure high sexual receptivity before mating. Mating was induced on Day 2,9 and16. PPT data was analyzed using TimeSSI1 for social interaction test system (O' Hara & Co., Ltd.). Briefly, the experimental subject was placed in a chamber, in which two pen-boxes (diameter 8cm, height10cm) were located at two diagonally opposite corners. The experimental animal was free to move throughout the chamber and the time spent in close proximity to each pen-box (stay time) is recorded

using an automated mouse tracking system (Fig.4 A, B). In the habituation phase, the experimental subject was allowed to explore the chamber for 5 minutes with both pen-boxes empty. In the recognition phase, the partner stimulus animal was restricted in one pen-box, and a novel "stranger" stimulus animal was restricted in another pen-box, and the experimental subject was allowed to explore the chamber for 10 minutes. In the preference phase, the positions of the partner stimulus animal and the "stranger" stimulus animal were switched, and the experimental subject was allowed to explore the chamber for 20 minutes. To assure unbiased design, pen-box assignments were counterbalanced for the diagonal positions. All of the experimenters were blind to the genotype of the subjects.

Parental behavior test

To examine maternal behavior, we performed pup retrieval test with virgin female mice (2- to 4-months old, 15-18mice/line), following the method described in [76] with some modifications. Briefly, 5 days prior to the behavioral testing, each subject was isolated and housed in separate home cages in the test room. Nesting material (about 1.5 g of cotton wool) was provided for nest making. The tests were conducted in the dark phase of light/dark cycle (12 hours/12 hours). On the day of the test, each subject was placed in the recording area and allowed 15 minutes for habituation. The stimulus pups (age: P2-P3) were collected from a group of donor mothers immediately before the start of the experiment. A retrieval test began with the placement of 3 stimulus pups on the side farthest form the nest, and the female's behavior was recorded by an ARNAN 4 channel security system for 15 minutes. Pup retrieval was defined as picking up the pup and bringing it to the nest. If the subject did not complete the retrieval for 3 pups in 15 minutes, the video recording time was extended to 30 minutes. The latency to retrieve each pup (1st, 2nd, 3rd) and the time spent crouching on the pups were time-stamped and calculated manually. A latency of 1800 seconds was assigned if the pup-retrieval was not completed in 30 minutes. Crouching was defined as the mouse supporting itself in a lactation-position over the pups in the nest. Crouching time on a single pup, two pups, and three pups were summed up as total crouching time. All of the experimenters were blind to the genotype of the subjects.

Statistical analysis

All the statistical analyses were performed by SPSS21(IBM). Mixed ANOVA was used for analyzing PPT data and pup retrieval data. Mauchly's test of sphericity was used to test whether or not the assumption of sphericity was met in repeated measures. Greenhouse-Geisser correction was applied when the sphericity was violated. Two-way ANOVA was used for analyzing qRT-PCR region specific data across different mouse lines. One-way ANOVA was used for analyzing crouching time in the parental behavioral test. If there was a significant main effect of an independent factor, post hoc test was used to do multiple comparisons. If there was a significant interaction between within-subject factor and between-subject factor, post hoc pairwise comparisons were applied to analyze the simple main effects. Bonferroni correction was used for all the post hoc tests.

Supplemental information titles and legends:

Supplementary Fig.1 Transgenic CRE mediated Lac-Z reporter gene expression in the brain of Koi lines. X-gal staining of the brains from the double positive (*Cre*+, *LacZ*+) offspring of Koi-5 (A-C), Koi-6 (D-F), Koi-7 (G-I), Koi-8 (J-L). Scale=1mm

Supplementary Fig.2 Negative control of whole-mount mammary gland staining. X-gal staining of a mammary gland from (*Cre*-, *LacZ*+) offspring from heterozygous Koi-4 was shown. The lymph node showed some blue signal, indicating that the lymph node could be stained nonspecifically. All the epithelium ducts did not show any blue signal, verifying the specificity of duct labeling of X-gal staining. Scale=500um

Supplementary Fig.3 Heatmap of the chromatin contacts surrounding *Oxtr* and *Oxt* across mouse tissues/cells from megabase-size visualization. (A) Heatmap of the chromatin contacts surrounding *Oxtr* across mouse tissues/cells: *Oxtr* is located at a TAD boundary region. The increase of interactions characterizes the TADs structure and the interaction of two neighboring TADs can be more clearly observed in brain-related samples. Blue dashed lines were prepared to help observing the TAD structures, and black circles were prepared to help observing the long-distance interaction obtained from Hi-C interaction matrices surrounding *Oxtr*. (B) Heatmap of the chromatin contacts surrounding *Oxt* across mouse tissues/cells. No TAD structure was observed surrounding *Oxt* locus.

Supplementary Fig.4 Heatmap of the chromatin contacts surrounding *OXTR* and *OXT* across human tissues/cells from megabase-size visualization.

(A) Heatmap of the chromatin contacts surrounding *OXTR* across human tissues/cells. The human *OXTR* is also located at a TAD boundary region. Blue dashed lines were prepared to help observing the large TAD structure obtained from Hi-C interaction matrices. (B) Heatmap of the chromatin contacts surrounding *OXT* across human tissues/cells. No typical TAD structure was observed surrounding *OXT* locus.

Supplementary Fig.5 Quantitative PCR analysis of *Oxtr* mRNA expression in different brain regions revealed by common primer set recognizing both m*Oxtr* and pv*Oxtr*. qPCR was used to analyzed Oxtr mRNA in olfactory bulb, prefrontal cortex, striatum and thalamus from WT, Koi-1, Koi-2, Koi-3, Koi-4 and *mOxtr*$^{-/-}$ mutant mice, n=4 for each genotype. Note that the level of *Oxtr* mRNA in *mOxtr*$^{-/-}$ mutant mice was nondetectable (ND). The autoradiograph of OXTR binding in olfactory bulb from each line were shown alongside the legend. There was a significant interaction between position and genotype $F(12,64) = 26.33$, $p<0.0001$; Post hoc Bonferroni test revealed that *Oxtr* expression level in olfactory bulb of Koi-1 was significantly higher than that of other genotype groups ($p<0.0001$ for all), and that of Koi-4 was significantly higher than that of Koi-3 $p<0.05$. And the striatum of Koi-4 expressed significantly higher *Oxtr* when compared with WT and Koi-3($p<0.05$ for both). The *Oxtr* expression level in thalamus of Koi-4 was significantly higher than other genotype groups ($p<0.0001$ when compared with WT and Koi-3, $p<0.001$ when compared with Koi-2, $p<0.05$ when comparedg with Koi-1.) Significance of interaction between genotype and brain region: # # # # $p<0.0001$. The significance of single main effect of genotype: * $p<0.05$; * * $p<0.01$; * * * $p<0.001$; * * * * $p<0.0001$.

Supplementary Fig.6 Quantitative analysis of *Oxtr* mRNA expression in different brain regions revealed by a primer set specifically recognizing pv*Oxtr*. The tissue of olfactory bulb, prefrontal cortex, striatum and thalamus from WT, Koi-1, Koi-2, Koi-3 and Koi-4 mice were analyzed, n=4 for each genotype. Note that the level of *Oxtr* mRNA in WT mice was barely detectable. There was a significant interaction between position and genotype $F(9,48) = 89.25$, $p<0.0001$; Post Hoc Bonferroni test revealed that *Oxtr* expression level in the olfactory bulb of Koi-1 was significantly higher than that of other genotype groups ($p<0.0001$ for all), and that of Koi-4 was significantly higher than that of Koi-2 and Koi-3 ($p<0.0001$ for both). The *Oxtr* expression level in prefrontal cortex of Koi-3 was significantly higher than that of other groups ($p<0.01$ when comparing with Koi-1 and Koi-4; $p<0.05$ when comparing with Koi-2). And the striatum of Koi-4 expressed significantly higher *Oxtr* when comparing with Koi-2 and Koi-3

(p<0.01 for both). The *Oxtr* expression level in thalamus of Koi-4 was significantly higher than that of other genotype groups (p<0.0001 for all). The significance of interaction between genotype and brain region: # # # # p<0.0001. The significance of single main effect of genotype: * p<0.05; * * p<0.01; * * * p<0.001; * * * * p<0.0001.

Supplementary Table.1

The datasets IDs and sample information for mouse 3D chromatin verification

The database source of each mouse sample, analysis and visualization tool information, and the region analyzed was listed.

Supplementary Table.2

The datasets IDs and sample information for human 3D chromatin verification

The database source of each human sample, analysis and visualization tool information, and the region analyzed was listed.

References:

1. Jurek, B., and Neumann, I.D. (2018). The Oxytocin Receptor: From Intracellular Signaling to Behavior. Physiol Rev *98*, 1805-1908.
2. Froemke, R.C., and Young, L.J. (2021). Oxytocin, Neural Plasticity, and Social Behavior. Annu Rev Neurosci *44*, 359-381.
3. Rigney, N., de Vries, G.J., Petrulis, A., and Young, L.J. (2022). Oxytocin, Vasopressin, and Social Behavior: From Neural Circuits to Clinical Opportunities. Endocrinology *163*.
4. Young, L.J., and Zhang, Q.I. (2021). On the Origins of Diversity in Social Behavior. The Japanese Journal of Animal Psychology *doi: 10.2502/janip.71.1.4*.
5. Barrett, C.E., Arambula, S.E., and Young, L.J. (2015). The oxytocin system promotes resilience to the effects of neonatal isolation on adult social attachment in female prairie voles. Transl Psychiatry *5*, e606.
6. Ahern, T.H., Olsen, S., Tudino, R., and Beery, A.K. (2021). Natural variation in the oxytocin receptor gene and rearing interact to influence reproductive and nonreproductive social behavior and receptor binding. Psychoneuroendocrinology *128*, 105209.
7. Ross, H.E., Freeman, S.M., Spiegel, L.L., Ren, X., Terwilliger, E.F., and Young, L.J. (2009). Variation in oxytocin receptor density in the nucleus accumbens has differential effects on affiliative behaviors in monogamous and polygamous voles. J Neurosci *29*, 1312-1318.

8. King, L.B., Walum, H., Inoue, K., Eyrich, N.W., and Young, L.J. (2016). Variation in the Oxytocin Receptor Gene Predicts Brain Region-Specific Expression and Social Attachment. Biol Psychiatry *80*, 160-169.
9. Rogers Flattery, C.N., Coppeto, D.J., Inoue, K., Rilling, J.K., Preuss, T.M., and Young, L.J. (2022). Distribution of brain oxytocin and vasopressin V1a receptors in chimpanzees (Pan troglodytes): comparison with humans and other primate species. Brain Struct Funct *227*, 1907-1919.
10. Skuse, D.H., Lori, A., Cubells, J.F., Lee, I., Conneely, K.N., Puura, K., Lehtimäki, T., Binder, E.B., and Young, L.J. (2014). Common polymorphism in the oxytocin receptor gene (OXTR) is associated with human social recognition skills. Proceedings of the National Academy of Sciences *111*, 1987-1992.
11. Theofanopoulou, C., Andirkó, A., Boeckx, C., and Jarvis, E.D. (2022). Oxytocin and vasotocin receptor variation and the evolution of human prosociality. Comprehensive Psychoneuroendocrinology *11*, 100139.
12. Keebaugh, A.C., and Young, L.J. (2011). Increasing oxytocin receptor expression in the nucleus accumbens of pre-pubertal female prairie voles enhances alloparental responsiveness and partner preference formation as adults. Horm Behav *60*, 498-504.
13. Keebaugh, A.C., Barrett, C.E., Laprairie, J.L., Jenkins, J.J., and Young, L.J. (2015). RNAi knockdown of oxytocin receptor in the nucleus accumbens inhibits social attachment and parental care in monogamous female prairie voles. Soc Neurosci *10*, 561-570.
14. Berendzen, K.M., Sharma, R., Mandujano, M.A., Wei, Y., Rogers, F.D., Simmons, T.C., Seelke, A.M.H., Bond, J.M., Larios, R., Goodwin, N.L., et al. (2023). Oxytocin receptor is not required for social attachment in prairie voles. Neuron *111*, 787-796.e784.
15. Mack, K.L., Campbell, P., and Nachman, M.W. (2016). Gene regulation and speciation in house mice. Genome Res *26*, 451-461.
16. Osada, N., Miyagi, R., and Takahashi, A. (2017). Cis- and Trans-regulatory Effects on Gene Expression in a Natural Population of Drosophila melanogaster. Genetics *206*, 2139-2148.
17. Shi, X., Ng, D.W.K., Zhang, C., Comai, L., Ye, W., and Jeffrey Chen, Z. (2012). Cis- and trans-regulatory divergence between progenitor species determines gene-expression novelty in Arabidopsis allopolyploids. Nature Communications *3*, 950.
18. Signor, S.A., and Nuzhdin, S.V. (2018). The Evolution of Gene Expression in cis and trans. Trends Genet *34*, 532-544.
19. Suster, M.L., Abe, G., Schouw, A., and Kawakami, K. (2011). Transposon-mediated BAC transgenesis in zebrafish. Nature Protocols *6*, 1998-2021.

20. Beil, J., Fairbairn, L., Pelczar, P., and Buch, T. (2012). Is BAC transgenesis obsolete? State of the art in the era of designer nucleases. J Biomed Biotechnol *2012*, 308414.
21. Bian, Q., and Belmont, A.S. (2010). BAC TG-EMBED: one-step method for high-level, copy-number-dependent, position-independent transgene expression. Nucleic Acids Research *38*, e127-e127.
22. Schmidt, E.F., Kus, L., Gong, S., and Heintz, N. (2013). BAC transgenic mice and the GENSAT database of engineered mouse strains. Cold Spring Harb Protoc *2013*.
23. Gerfen, C.R., Paletzki, R., and Heintz, N. (2013). GENSAT BAC cre-recombinase driver lines to study the functional organization of cerebral cortical and basal ganglia circuits. Neuron *80*, 1368-1383.
24. Heintz, N. (2004). Gene Expression Nervous System Atlas (GENSAT). Nature Neuroscience *7*, 483-483.
25. Gong, S., Doughty, M., Harbaugh, C.R., Cummins, A., Hatten, M.E., Heintz, N., and Gerfen, C.R. (2007). Targeting Cre recombinase to specific neuron populations with bacterial artificial chromosome constructs. J Neurosci *27*, 9817-9823.
26. Ferrante, R.J. (2009). Mouse models of Huntington's disease and methodological considerations for therapeutic trials. Biochimica et Biophysica Acta (BBA) - Molecular Basis of Disease *1792*, 506-520.
27. Shenoy, S.A., Zheng, S., Liu, W., Dai, Y., Liu, Y., Hou, Z., Mori, S., Tang, Y., Cheng, J., Duan, W., et al. (2022). A novel and accurate full-length HTT mouse model for Huntington's disease. Elife *11*, e70217.
28. Crook, Z.R., and Housman, D. (2011). Huntington's disease: can mice lead the way to treatment? Neuron *69*, 423-435.
29. Taguchi, T., Ikuno, M., Hondo, M., Parajuli, L.K., Taguchi, K., Ueda, J., Sawamura, M., Okuda, S., Nakanishi, E., Hara, J., et al. (2019). α-Synuclein BAC transgenic mice exhibit RBD-like behaviour and hyposmia: a prodromal Parkinson's disease model. Brain *143*, 249-265.
30. Yang, X.W., and Lu, X.-H. (2008). Chapter 19 - The Bac Transgenic Approach to Study Parkinson's Disease in Mice. In Parkinson's Disease, R. Nass and S. Przedborski, eds. (San Diego: Academic Press), pp. 247-268.
31. McGraw, L.A., Davis, J.K., Lowman, J.J., ten Hallers, B.F.H., Koriabine, M., Young, L.J., de Jong, P.J., Rudd, M.K., and Thomas, J.W. (2010). Development of genomic resources for the prairie vole (Microtus ochrogaster): construction of a BAC library and vole-mouse comparative cytogenetic map. BMC Genomics *11*, 70.
32. McGraw, L.A., Davis, J.K., Thomas, P.J., Young, L.J., and Thomas, J.W. (2012). BAC-based sequencing of behaviorally-relevant genes in the prairie vole. PLoS One *7*, e29345.

909 33. Zhang, Q., Sano, C., Masuda, A., Ando, R., Tanaka, M., and Itohara, S. (2016). Netrin-G1
910 regulates fear-like and anxiety-like behaviors in dissociable neural circuits. Scientific
911 Reports *6*, 28750.
912 34. Kandasamy, L.C., Tsukamoto, M., Banov, V., Tsetsegee, S., Nagasawa, Y., Kato, M.,
913 Matsumoto, N., Takeda, J., Itohara, S., Ogawa, S., et al. (2021). Limb-clasping, cognitive
914 deficit and increased vulnerability to kainic acid-induced seizures in neuronal
915 glycosylphosphatidylinositol deficiency mouse models. Human Molecular Genetics *30*,
916 758-770.
917 35. Newmaster, K.T., Nolan, Z.T., Chon, U., Vanselow, D.J., Weit, A.R., Tabbaa, M.,
918 Hidema, S., Nishimori, K., Hammock, E.A.D., and Kim, Y. (2020). Quantitative cellular-
919 resolution map of the oxytocin receptor in postnatally developing mouse brains. Nature
920 Communications *11*, 1885.
921 36. Inoue, K., Ford, C.L., Horie, K., and Young, L.J. (2022). Oxytocin receptors are widely
922 distributed in the prairie vole (Microtus ochrogaster) brain: Relation to social behavior,
923 genetic polymorphisms, and the dopamine system. Journal of Comparative Neurology *530*,
924 2881-2900.
925 37. Smirnov, A., Fishman, V., Yunusova, A., Korablev, A., Serova, I., Skryabin, B.V.,
926 Rozhdestvensky, T.S., and Battulin, N. (2019). DNA barcoding reveals that injected
927 transgenes are predominantly processed by homologous recombination in mouse zygote.
928 Nucleic Acids Research *48*, 719-735.
929 38. Chandler, K.J., Chandler, R.L., Broeckelmann, E.M., Hou, Y., Southard-Smith, E.M., and
930 Mortlock, D.P. (2007). Relevance of BAC transgene copy number in mice: transgene copy
931 number variation across multiple transgenic lines and correlations with transgene integrity
932 and expression. Mamm Genome *18*, 693-708.
933 39. Dekker, J., Rippe, K., Dekker, M., and Kleckner, N. (2002). Capturing chromosome
934 conformation. Science *295*, 1306-1311.
935 40. Dixon, J.R., Selvaraj, S., Yue, F., Kim, A., Li, Y., Shen, Y., Hu, M., Liu, J.S., and Ren, B.
936 (2012). Topological domains in mammalian genomes identified by analysis of chromatin
937 interactions. Nature *485*, 376-380.
938 41. Rajderkar, S., Barozzi, I., Zhu, Y., Hu, R., Zhang, Y., Li, B., Alcaina Caro, A., Fukuda-
939 Yuzawa, Y., Kelman, G., Akeza, A., et al. (2023). Topologically associating domain
940 boundaries are required for normal genome function. Communications Biology *6*, 435.
941 42. Beagan, J.A., and Phillips-Cremins, J.E. (2020). On the existence and functionality of
942 topologically associating domains. Nature Genetics *52*, 8-16.
943 43. Lieberman-Aiden, E., van Berkum, N.L., Williams, L., Imakaev, M., Ragoczy, T., Telling,
944 A., Amit, I., Lajoie, B.R., Sabo, P.J., Dorschner, M.O., et al. (2009). Comprehensive

Mapping of Long-Range Interactions Reveals Folding Principles of the Human Genome. Science *326*, 289-293.

44. Gibcus, Johan H., and Dekker, J. (2013). The Hierarchy of the 3D Genome. Molecular Cell *49*, 773-782.

45. Tribollet, E., Charpak, S., Schmidt, A., Dubois-Dauphin, M., and Dreifuss, J.J. (1989). Appearance and transient expression of oxytocin receptors in fetal, infant, and peripubertal rat brain studied by autoradiography and electrophysiology. J Neurosci *9*, 1764-1773.

46. Inoue, K., Ford, C.L., Horie, K., and Young, L.J. Oxytocin receptors are widely distributed in the prairie vole (Microtus ochrogaster) brain: Relation to social behavior, genetic polymorphisms, and the dopamine system. Journal of Comparative Neurology *n/a*.

47. Walum, H., and Young, L.J. (2018). The neural mechanisms and circuitry of the pair bond. Nat Rev Neurosci *19*, 643-654.

48. Olazábal, D.E., and Young, L.J. (2006). Oxytocin receptors in the nucleus accumbens facilitate "spontaneous" maternal behavior in adult female prairie voles. Neuroscience *141*, 559-568.

49. Carcea, I., Caraballo, N.L., Marlin, B.J., Ooyama, R., Riceberg, J.S., Mendoza Navarro, J.M., Opendak, M., Diaz, V.E., Schuster, L., Alvarado Torres, M.I., et al. (2021). Oxytocin neurons enable social transmission of maternal behaviour. Nature *596*, 553-557.

50. Marlin, B.J., Mitre, M., D'Amour J, A., Chao, M.V., and Froemke, R.C. (2015). Oxytocin enables maternal behaviour by balancing cortical inhibition. Nature *520*, 499-504.

51. Olazábal, D.E., and Young, L.J. (2006). Species and individual differences in juvenile female alloparental care are associated with oxytocin receptor density in the striatum and the lateral septum. Horm Behav *49*, 681-687.

52. Ophir, A.G., Gessel, A., Zheng, D.J., and Phelps, S.M. (2012). Oxytocin receptor density is associated with male mating tactics and social monogamy. Horm Behav *61*, 445-453.

53. Walum, H., and Young, L.J. (2018). The neural mechanisms and circuitry of the pair bond. Nature Reviews Neuroscience *19*, 643-654.

54. Amadei, E.A., Johnson, Z.V., Jun Kwon, Y., Shpiner, A.C., Saravanan, V., Mays, W.D., Ryan, S.J., Walum, H., Rainnie, D.G., Young, L.J., et al. (2017). Dynamic corticostriatal activity biases social bonding in monogamous female prairie voles. Nature *546*, 297-301.

55. Shapiro, L.E., and Insel, T.R. (1989). Ontogeny of oxytocin receptors in rat forebrain: a quantitative study. Synapse *4*, 259-266.

56. Tribollet, E., Charpak, S., Schmidt, A., Dubois-Dauphin, M., and Dreifuss, J. (1989). Appearance and transient expression of oxytocin receptors in fetal, infant, and

peripubertal rat brain studied by autoradiography and electrophysiology. The Journal of Neuroscience *9*, 1764-1773.

57. Hammock, E.A., and Levitt, P. (2013). Oxytocin receptor ligand binding in embryonic tissue and postnatal brain development of the C57BL/6J mouse. Front Behav Neurosci *7*, 195.

58. Nardou, R., Lewis, E.M., Rothhaas, R., Xu, R., Yang, A., Boyden, E., and Dölen, G. (2019). Oxytocin-dependent reopening of a social reward learning critical period with MDMA. Nature *569*, 116-120.

59. Hammock, E.A.D. (2015). Developmental Perspectives on Oxytocin and Vasopressin. Neuropsychopharmacology *40*, 24-42.

60. Young, L.J., and Crews, D. (1995). Comparative neuroendocrinology of steroid receptor gene expression and regulation: Relationship to physiology and behavior. Trends Endocrinol Metab *6*, 317-323.

61. Ross, H.E., and Young, L.J. (2009). Oxytocin and the neural mechanisms regulating social cognition and affiliative behavior. Front Neuroendocrinol *30*, 534-547.

62. Venkatesh, B., Si-Hoe, S.L., Murphy, D., and Brenner, S. (1997). Transgenic rats reveal functional conservation of regulatory controls between the Fugu isotocin and rat oxytocin genes. Proc Natl Acad Sci U S A *94*, 12462-12466.

63. Gilligan, P., Brenner, S., and Venkatesh, B. (2003). Neurone-specific expression and regulation of the pufferfish isotocin and vasotocin genes in transgenic mice. J Neuroendocrinol *15*, 1027-1036.

64. Knobloch, H.S., Charlet, A., Hoffmann, Lena C., Eliava, M., Khrulev, S., Cetin, Ali H., Osten, P., Schwarz, Martin K., Seeburg, Peter H., Stoop, R., et al. (2012). Evoked Axonal Oxytocin Release in the Central Amygdala Attenuates Fear Response. Neuron *73*, 553-566.

65. Gong, S., Zheng, C., Doughty, M.L., Losos, K., Didkovsky, N., Schambra, U.B., Nowak, N.J., Joyner, A., Leblanc, G., Hatten, M.E., et al. (2003). A gene expression atlas of the central nervous system based on bacterial artificial chromosomes. Nature *425*, 917-925.

66. Gawenis, L.R., Hodges, C.A., McHugh, D.R., Valerio, D.M., Miron, A., Cotton, C.U., Liu, J., Walker, N.M., Strubberg, A.M., Gillen, A.E., et al. (2019). A BAC Transgene Expressing Human CFTR under Control of Its Regulatory Elements Rescues Cftr Knockout Mice. Scientific Reports *9*, 11828.

67. Xiao, J.Y., Hafner, A., and Boettiger, A.N. (2021). How subtle changes in 3D structure can create large changes in transcription. Elife *10*, e64320.

68. Lee, M., Lori, A., Langford, N.A., and Rilling, J.K. (2022). Enhanced endogenous oxytocin signaling in the brain modulates neural responses to social misalignment and promotes

conformity in humans: A multi-locus genetic profile approach. Psychoneuroendocrinology *144*, 105869.

69. Hernandez, L.M., Lawrence, K.E., Padgaonkar, N.T., Inada, M., Hoekstra, J.N., Lowe, J.K., Eilbott, J., Jack, A., Aylward, E., Gaab, N., et al. (2020). Imaging-genetics of sex differences in ASD: distinct effects of OXTR variants on brain connectivity. Transl Psychiatry *10*, 82.

70. Vietri Rudan, M., Barrington, C., Henderson, S., Ernst, C., Odom, Duncan T., Tanay, A., and Hadjur, S. (2015). Comparative Hi-C Reveals that CTCF Underlies Evolution of Chromosomal Domain Architecture. Cell Reports *10*, 1297-1309.

71. Kim, J.H., Lee, S.R., Li, L.H., Park, H.J., Park, J.H., Lee, K.Y., Kim, M.K., Shin, B.A., and Choi, S.Y. (2011). High cleavage efficiency of a 2A peptide derived from porcine teschovirus-1 in human cell lines, zebrafish and mice. PLoS One *6*, e18556.

72. Hidema, S., Fukuda, T., Hiraoka, Y., Mizukami, H., Hayashi, R., Otsuka, A., Suzuki, S., Miyazaki, S., and Nishimori, K. (2016). Generation of Oxtr cDNA(HA)-Ires-Cre Mice for Gene Expression in an Oxytocin Receptor Specific Manner. J Cell Biochem *117*, 1099-1111.

73. Takayanagi, Y., Yoshida, M., Bielsky, I.F., Ross, H.E., Kawamata, M., Onaka, T., Yanagisawa, T., Kimura, T., Matzuk, M.M., Young, L.J., et al. (2005). Pervasive social deficits, but normal parturition, in oxytocin receptor-deficient mice. Proceedings of the National Academy of Sciences *102*, 16096-16101.

74. Wang, Y., Song, F., Zhang, B., Zhang, L., Xu, J., Kuang, D., Li, D., Choudhary, M.N.K., Li, Y., Hu, M., et al. (2018). The 3D Genome Browser: a web-based browser for visualizing 3D genome organization and long-range chromatin interactions. Genome Biol *19*, 151.

75. Li, D., Purushotham, D., Harrison, J.K., Hsu, S., Zhuo, X., Fan, C., Liu, S., Xu, V., Chen, S., Xu, J., et al. (2022). WashU Epigenome Browser update 2022. Nucleic Acids Research *50*, W774-W781.

76. Stolzenberg, D.S., Stevens, J.S., and Rissman, E.F. (2012). Experience-facilitated improvements in pup retrieval; evidence for an epigenetic effect. Horm Behav *62*, 128-135.

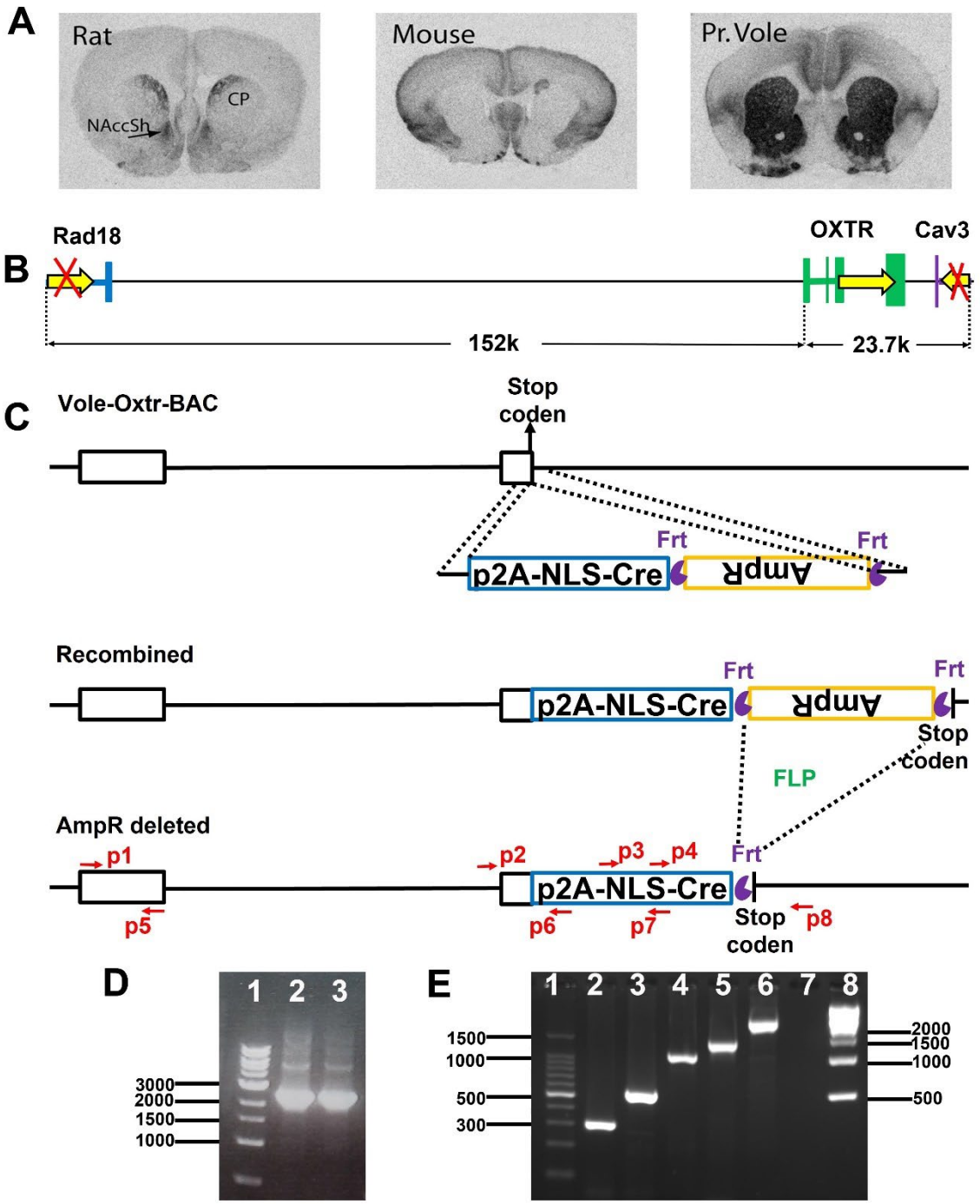

Fig.1 The construction of Koi lines

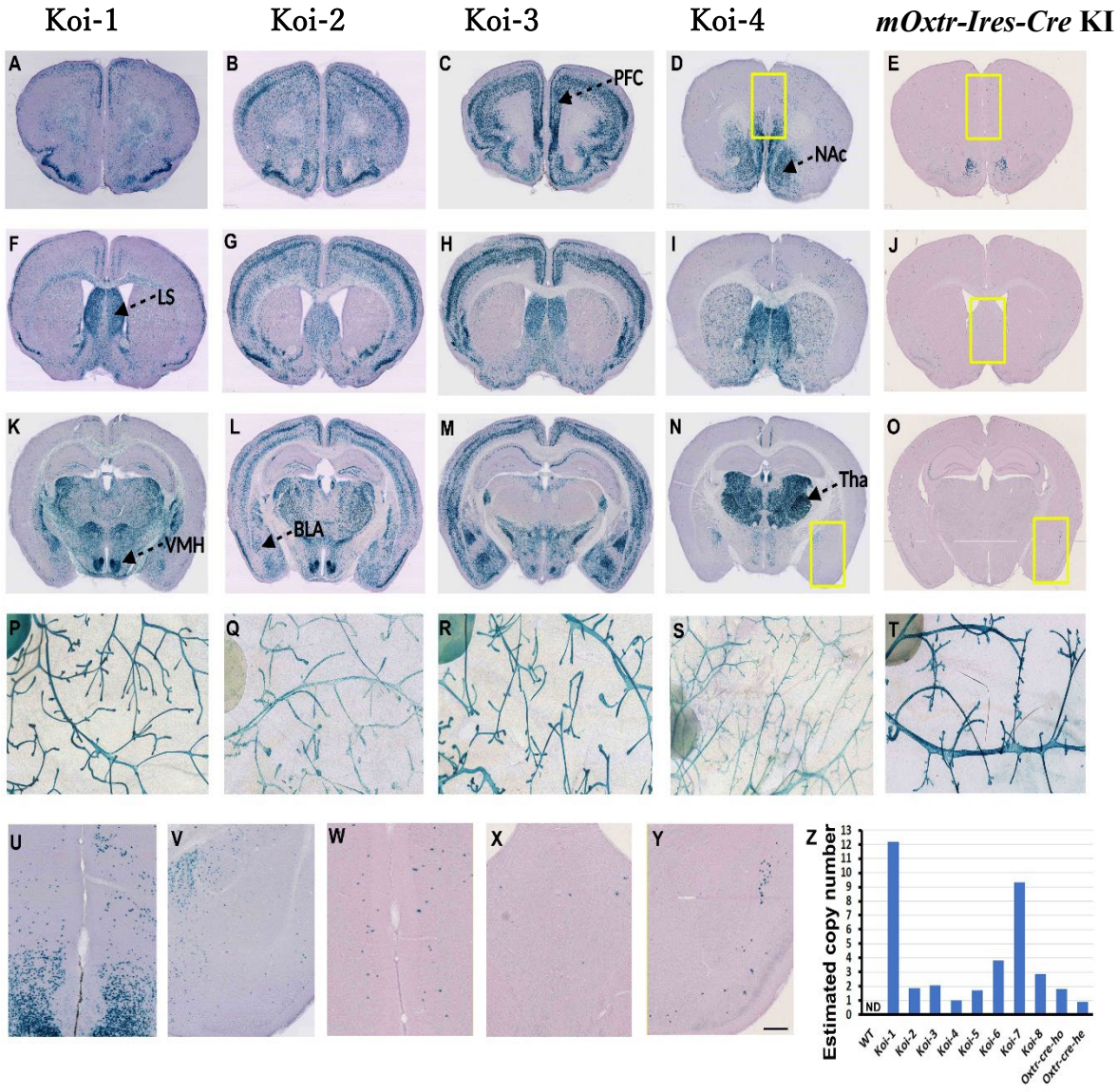

Fig.2 Transgenic CRE mediated Lac-Z reporter gene expression in the brain and mammary gland of Koi lines.

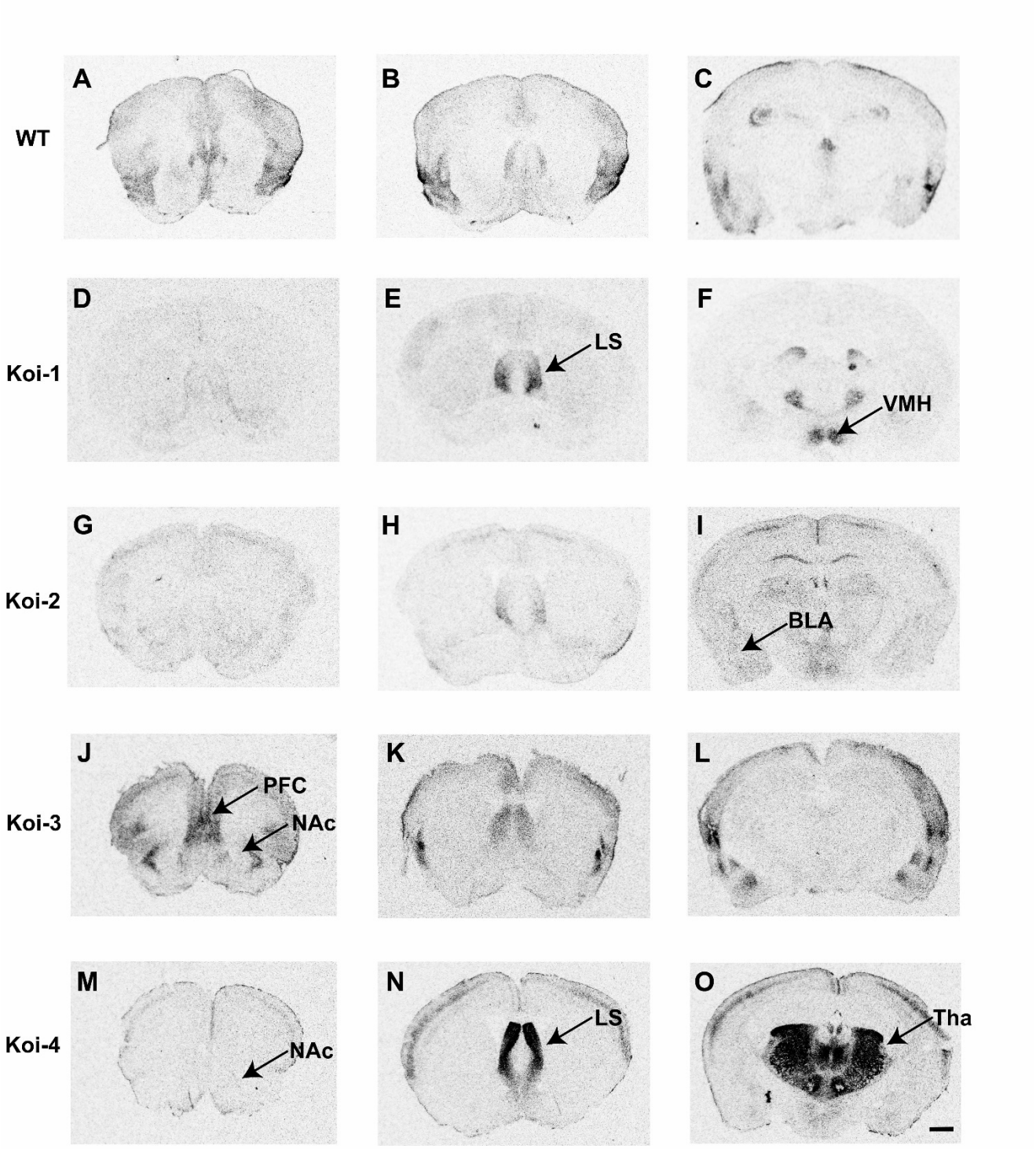

Fig.3The expression of OXTR in the brain of Koi lines.

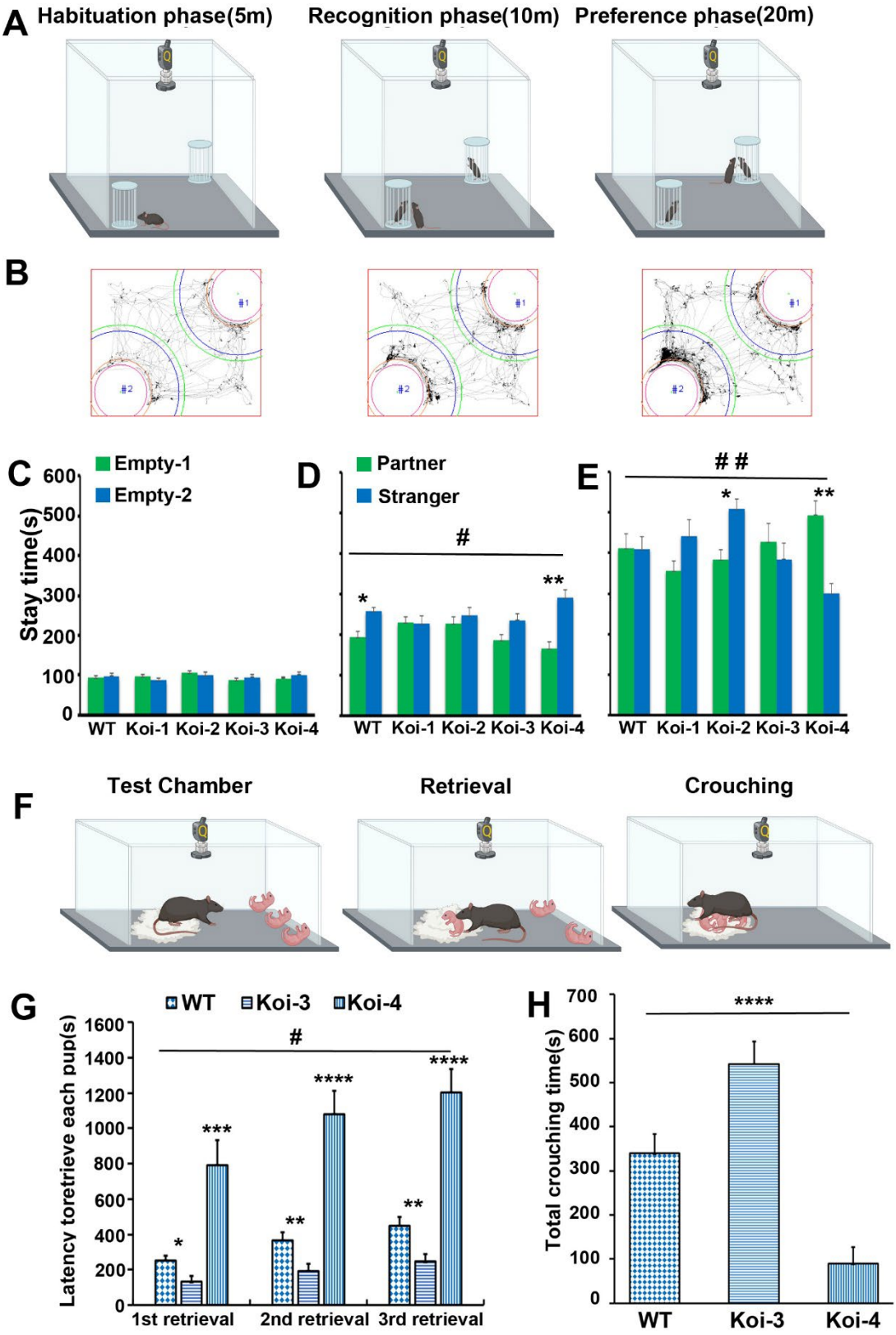

Fig.4 Social behaviors of Koi lines.

Supplementary Materials:

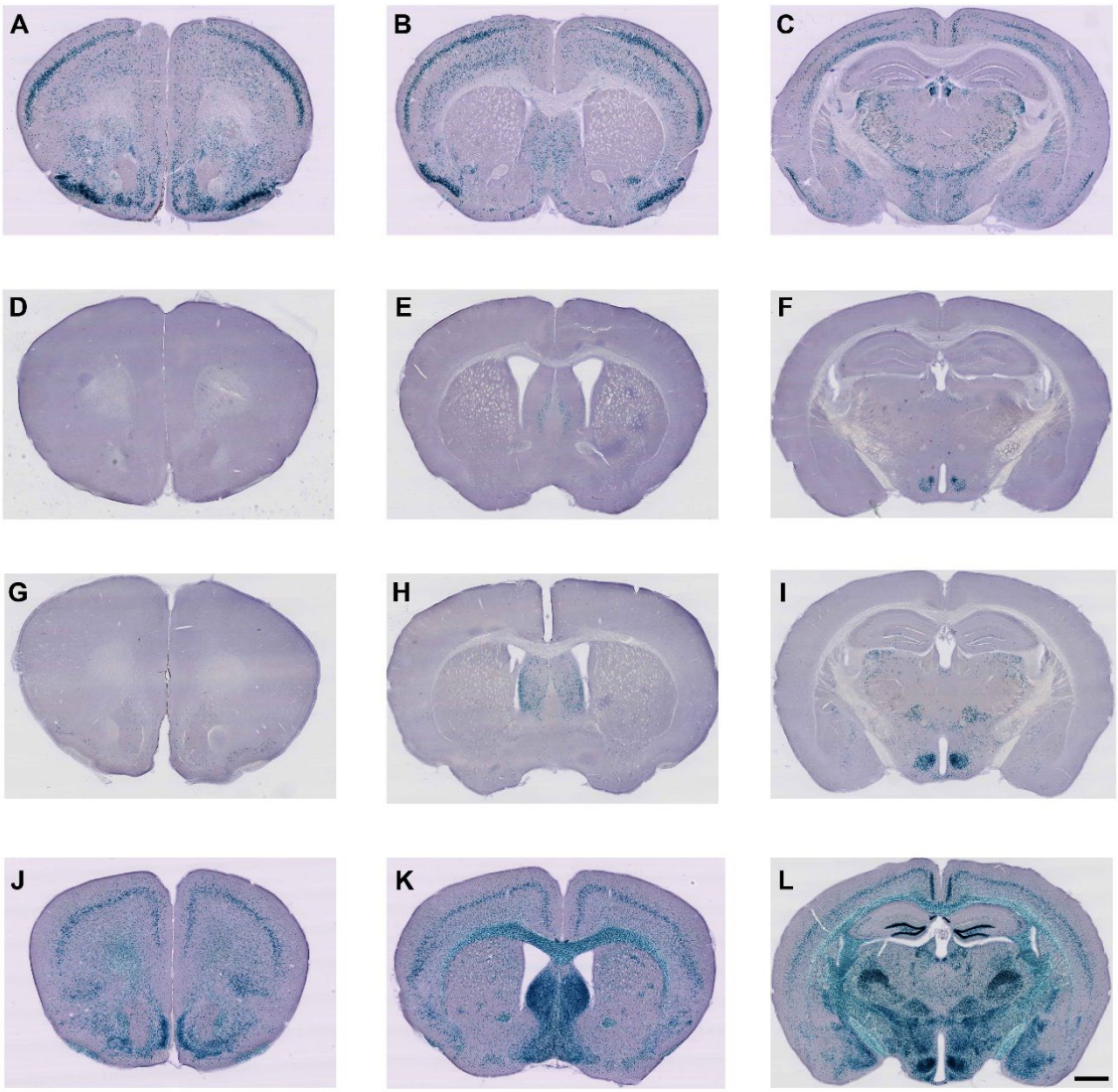

Supplementary Fig.1Transgenic CRE mediated Lac-Z reporter gene expression in the brain of Koi lines.

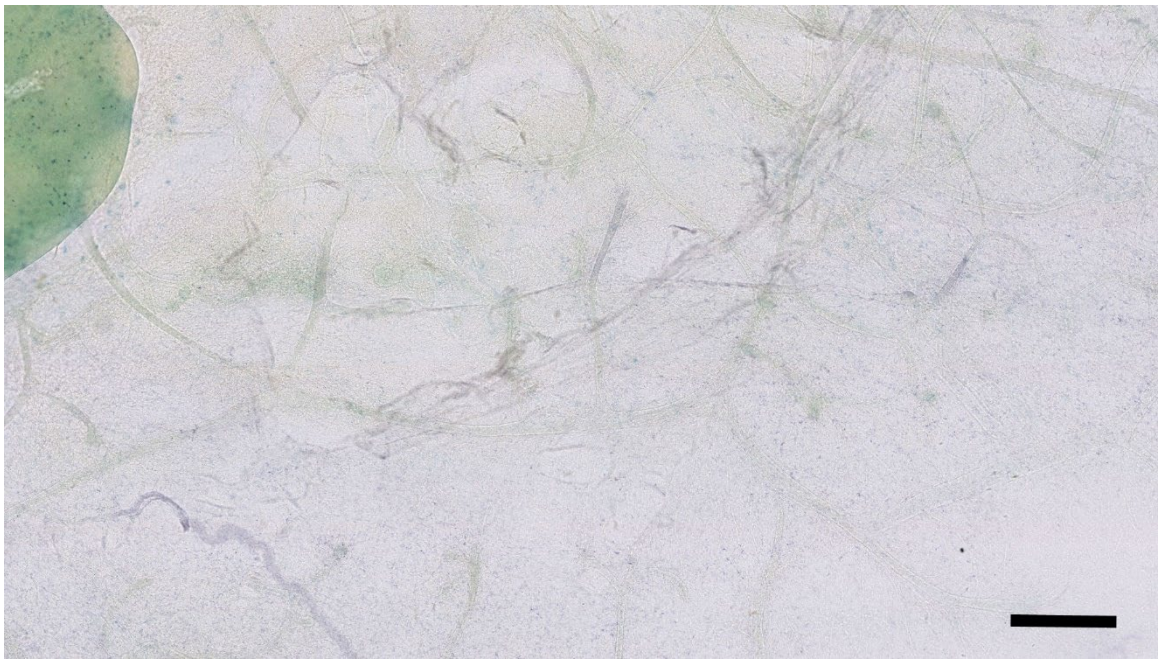

Supplementary Fig.2 Negative control of whole-mount mammary gland staining.

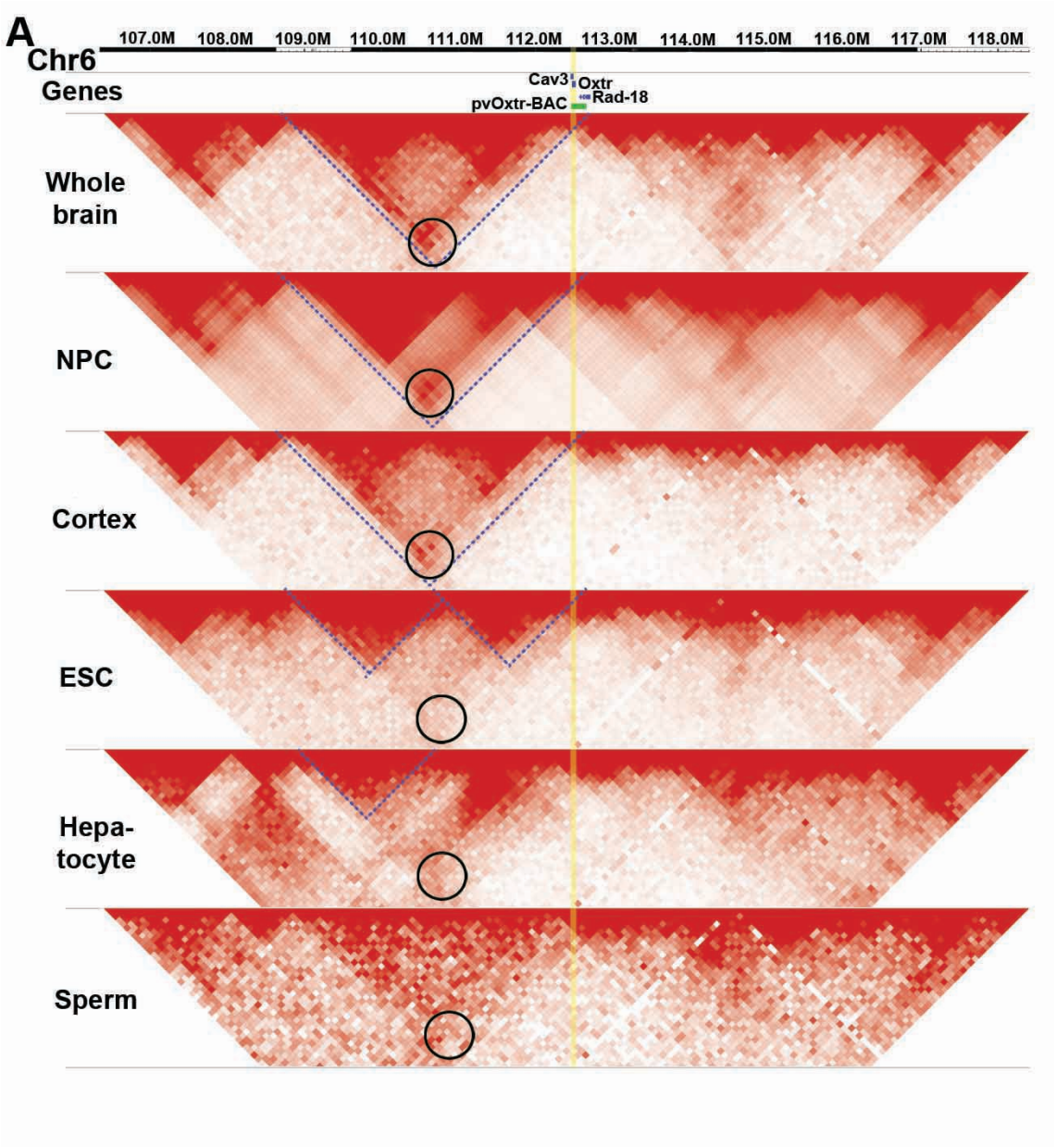

1089
1090
1091

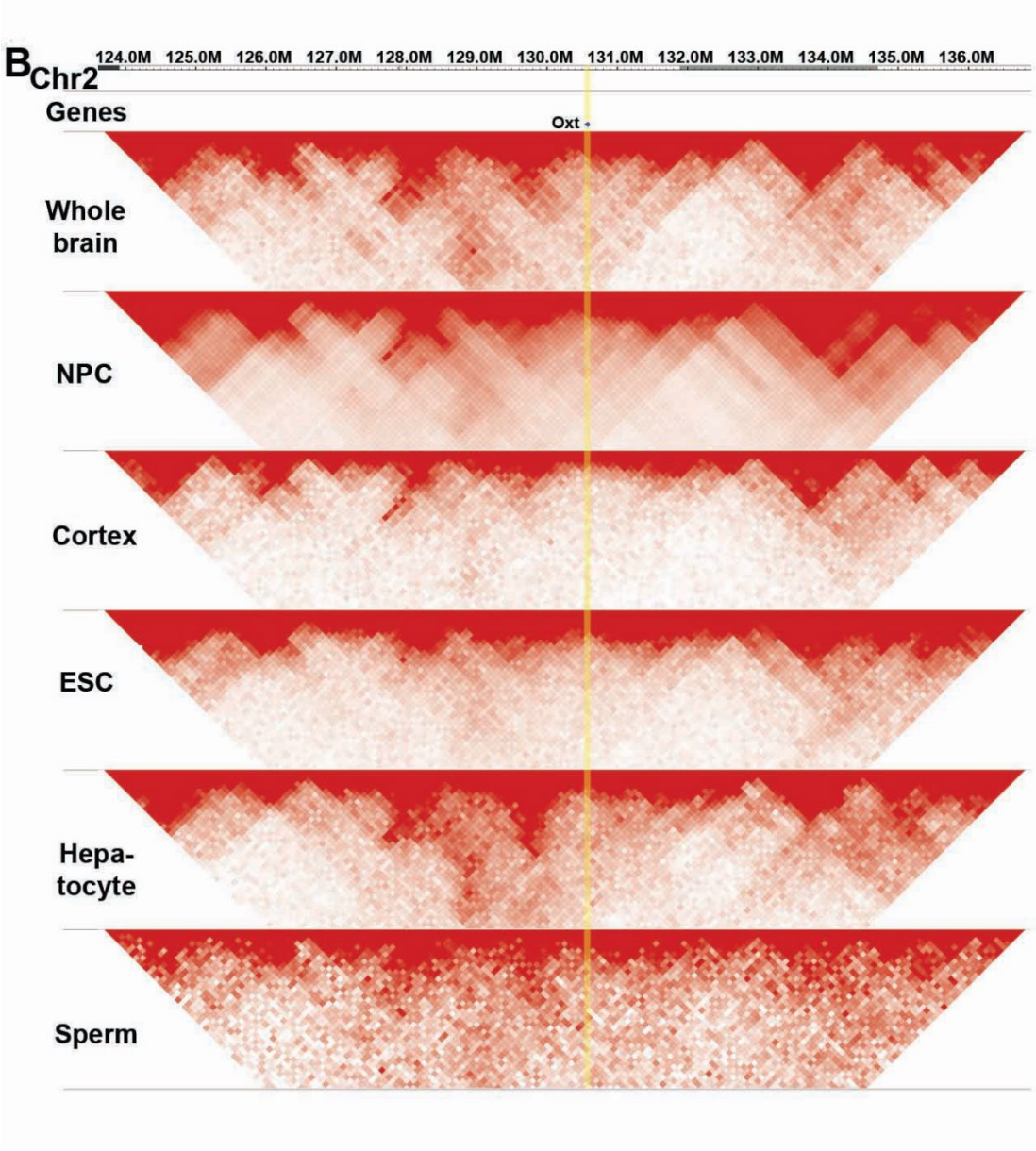

Supplementary Fig.3 Heatmap of the chromatin contacts surrounding *Oxtr* (A) and *Oxt* (B) across mouse tissues/cells from megabase-size visualization.

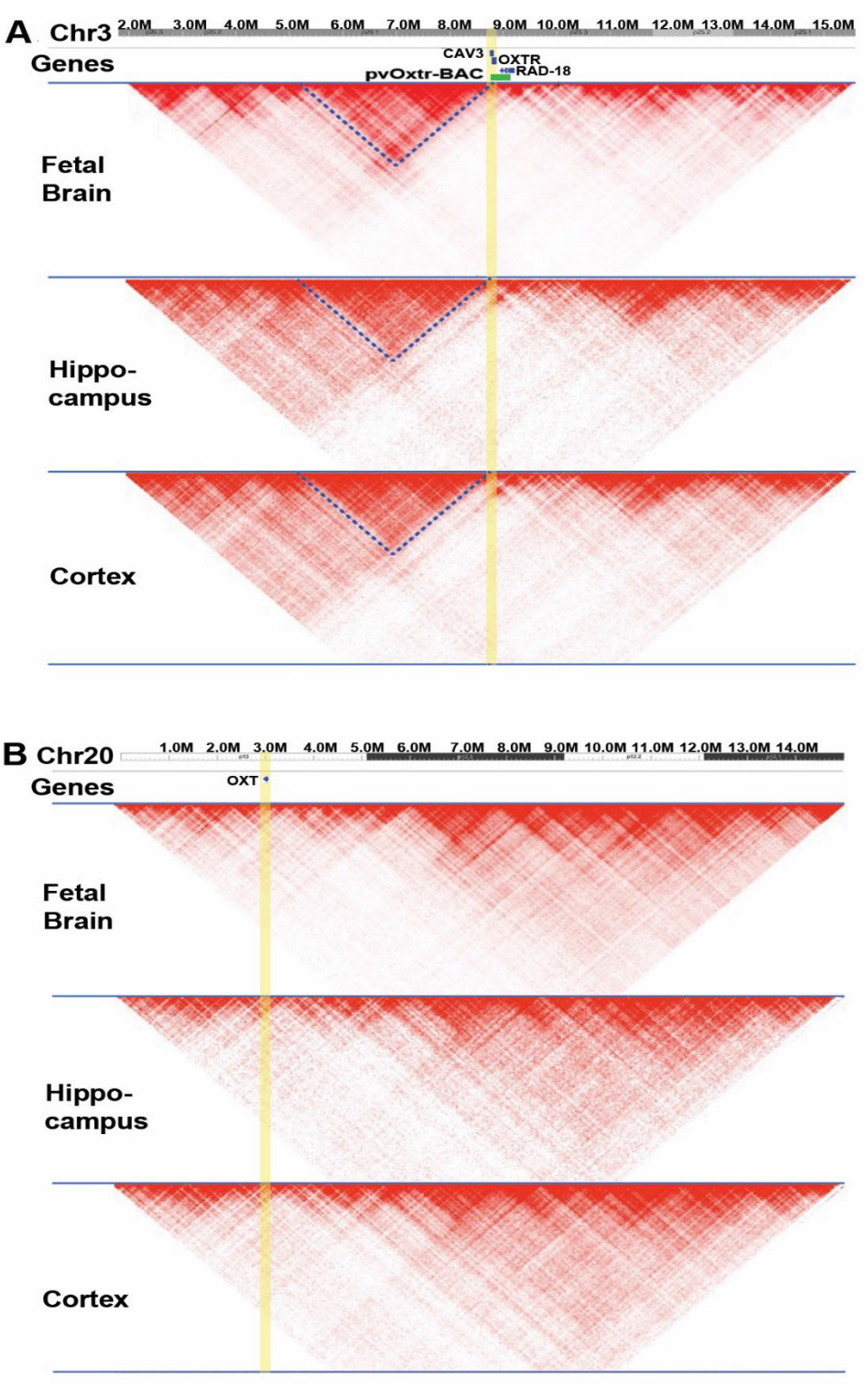

Supplementary Fig.4 Heatmap of the chromatin contacts surrounding *OXTR* (C) and *OXT* (D) across human tissues from megabase-size visualization.

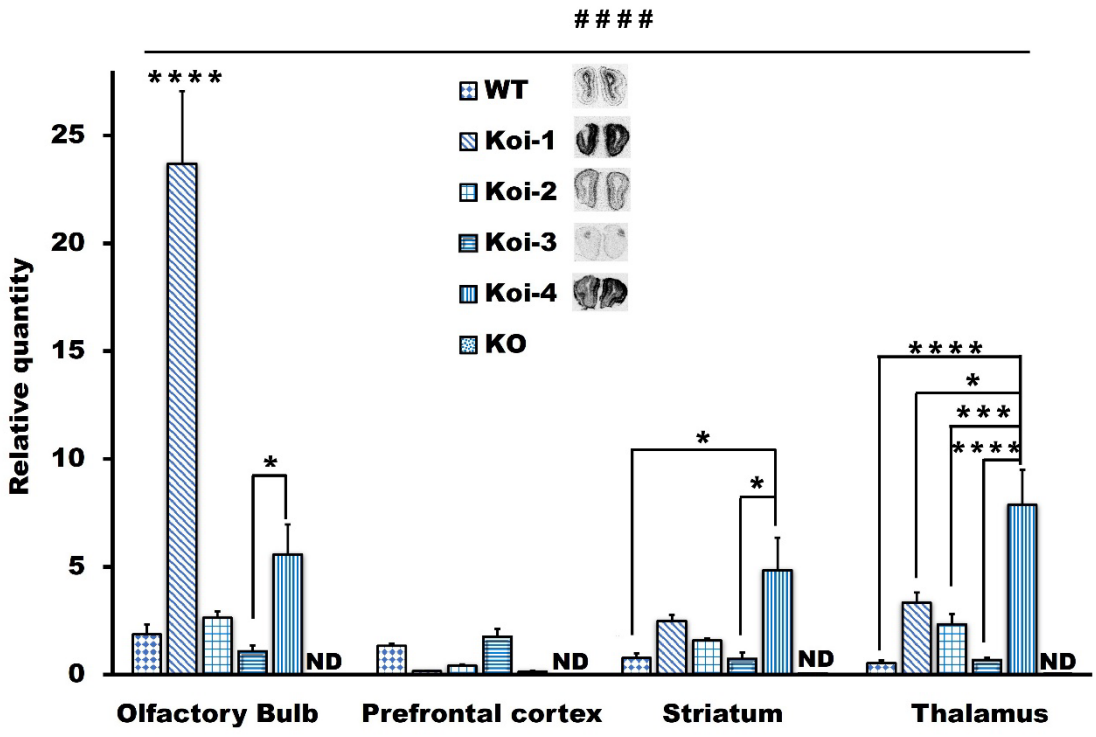

Supplementary Fig.5 Quantitative analysis of *Oxtr* mRNA expression in different brain regions revealed by common primer set recognizing both *mOxtr* and *pvOxtr*.

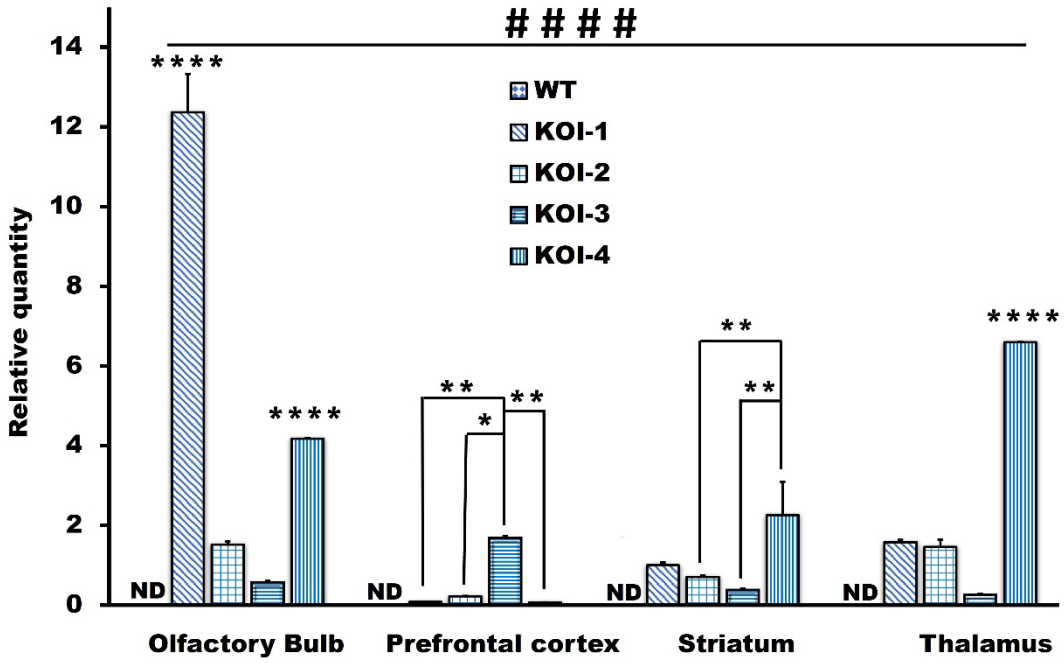

Supplementary Fig.6 Quantitative analysis of *Oxtr* mRNA expression in different brain regions revealed by a primer set specifically recognizing pv*Oxtr*.

	track	ID	Cell/tissue	Organism	Resolution	Restr. Enz.	Database	Database ID	Browser	Publication
Hi-C	1	Whole brain	whole brain	mm10	40 Kb	DNaseI	4DN	4DNFIQ48NYOW	WashU	Deng 2015
	2	NPC	NPC	mm10	40 Kb	DpnII	4DN	4DNFIHW8NTQX	WashU	Bonev 2017
	3	Cortex	cortex	mm10	40 Kb	MboI	4DN	4DNFII3JV8I1	WashU	Du 2017
	4	ESC	ESC	mm10	40 Kb	DpnII	4DN	4DNFIU8AF5ZY	WashU	Bonev 2017
	5	Hepatocyte	hepatocyte	mm10	40 Kb	HindIII	4DN	4DNFIFULDMGN	WashU	Schwarzer 2017
	6	Sperm	sperm	mm10	40 Kb	MboI	4DN	4DNFIN8F14CS	WashU	Du 2017
	Fig	Regions	Genes							
WashU	A	chr6:104149809-119528368	Oxtr							
	B	chr2:121804885-139358632	Oxt							

Supplementary Table.1

The datasets IDs and sample information for mouse 3D chromatin verification

	track	ID	Cell/tissue	Organism	Resolution	Database	Publication
Hi-C	1	Fetal brain	Fetal Brain GZ	hg19	10 Kb	3D genome	Won et al, 2016
	2	Hippocampus	Human hippocampus	hg19	40 Kb	3D genome	Schmitt et al., 2016
	3	Cortex	Cortex	hg19	40 Kb	3D genome	Schmitt et al., 2016
	Fig	Regions	Genes				
WashU	A	chr3:1831010-15559067	OXTR				
	B	chr20:0-15000000	OXT				

Supplementary Table.2

The datasets IDs and sample information for human 3D chromatin verification